Journal of Hydrology 641 (2024) 131773

Contents lists available at ScienceDirect

Journal of Hydrology

journal homepage: www.elsevier.com/locate/jhydrol

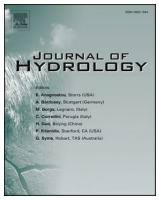

Research papers

Impact of surficial lithology on arsenic mobility in riverbanks of tidally fluctuating rivers: The Hooghly River, West Bengal, India

Kyungwon Kwak [a,*], Thomas S. Varner [b,*], Saptarshi Saha [c], Mesbah U. Bhuiyan [d], Harshad V. Kulkarni [b,e], Ananya Mukhopadhyay [c], Saugata Datta [b], Peter S. K. Knappett [a]

[a] Department of Geology and Geophysics, Texas A&M University, College Station, TX 77843, USA
[b] Department of Earth and Planetary Sciences, University of Texas at San Antonio, San Antonio, TX 78249, USA
[c] Department of Earth Sciences, Indian Institute of Engineering Science and Technology, Shibpur, Howrah, West Bengal 711103, India
[d] Department of Oceanography, Noakhali Science and Technology University, Noakhali 3814, Bangladesh
[e] School of Civil and Environmental Engineering, Indian Institute of Technology Mandi, Himachal Pradesh 175005, India

ARTICLE INFO

This manuscript was handled by Huaming Guo, Editor-in-Chief

Keywords:
Arsenic
Surface water-groundwater interactions
Hooghly River
Tidal river
Freshwater estuary

ABSTRACT

Arsenic (As) contamination in groundwater persists in South Asia. Precipitated amorphous Fe(III)-oxides regulate the mobilization of aqueous As and iron (Fe) within the hyporheic zone (HZ). Depending on the chemical stability of these Fe(III)-oxides, this so-called Natural Reactive Barrier (NRB) can function as a sink or source of aqueous As and Fe within shallow alluvial aquifers under influences of tidal and seasonal fluctuations of river stage. The extent to which surficial lithology influences the As mobility along a riverine (upstream) to tidal (downstream) continuum is uncertain. To explore this process along a tidally fluctuating river, two new study sites with contrasting surface lithology were characterized along the banks of Hooghly River. The upstream sandy riverbank aquifer experiences robust mixing with oxygen-rich surface water under influences of tidal fluctuations which maintain oxic conditions in the riverbank aquifer. Introduced riverine dissolved oxygen (DO) drives the in-situ precipitation of crystalline Fe(III)-oxides which remove dissolved As and Fe from groundwater before discharging to the river. Although sediment from the downstream silt-capped riverbank contains higher concentrations of sedimentary As and Fe compared to the sandy site, lower proportions of crystalline Fe(III)-oxide minerals were observed. Arsenic was more easily mobilized from the aluminosilicate clay minerals to which the As was primarily bound at the silt-capped riverbank, compared to the As bound to Fe(III)-oxides at the sandy site. Thus, aluminosilicates can be an important source of dissolved As. These findings demonstrate that the surficial lithology of a riverbank along a tidally and seasonally fluctuating river regulates the mobility of As and its mineralogical association within riverbank sediments in shallow riverbank aquifers.

1. Introduction

Shallow aquifers in the Bengal Basin's Ganga-Brahmaputra-Meghna (GBM) delta, stretching from West Bengal in India to Bangladesh, represent the most severe case of dissolved geogenic arsenic (As) contamination globally (Bhowmick et al., 2013; Chowdhury et al., 2000; DPHE/BGS, 2001; Fendorf et al., 2010; Nickson et al., 2000; Smedley and Kinniburgh, 2002; Smith et al., 2000). Despite decades of sustained efforts by governments, non-profit and inter-governmental organizations, and scientists to mitigate the As poisoning, the number of people (~100 million people) exposed to toxic concentrations of groundwater-borne As (>10 μg/L) remains relatively unchanged in South Asia (Chakraborti et al., 2009; Chakraborty et al., 2015; Human Rights Watch, 2016; Smith et al., 2000).

It is generally accepted that an important source of dissolved As in shallow aquifers in South and Southeast Asia is the microbially-mediated reductive dissolution of As-bearing Fe(III)-oxyhydroxide minerals (referred to herein as Fe(III)-oxides) (Fendorf et al., 2010; Harvey et al., 2002; Islam et al., 2004; Mailloux et al., 2013; McArthur et al., 2001; Nickson et al., 2000; Polizzotto et al., 2008; Smedley and Kinniburgh, 2002; Stahl et al., 2016; van Geen et al., 2004). However, the process of advective transport of reactants, such as dissolved organic carbon (DOC), to sites of reaction with solid-phase minerals, such as Fe (III)-oxides, and the advective transport of their products through

* Corresponding authors.
E-mail addresses: kkwak@tamu.edu (K. Kwak), tom.varner@my.utsa.edu (T.S. Varner).

https://doi.org/10.1016/j.jhydrol.2024.131773

Available online 6 August 2024

heterogeneous sedimentary layers produce a highly heterogeneous distribution of dissolved As concentrations (Aziz et al., 2008; Chakraborty et al., 2020, 2015; Kazmierczak et al., 2022; Mailloux et al., 2013; Polizzotto et al., 2008; Stahl et al., 2016; Xia et al., 2023).

In the Bengal Basin, ancient fluvial processes control the stratigraphy of the alluvial aquifers whereas recent fluvial processes shape land-surface morphology along current riverbanks (Goodbred et al., 2003; Kuehl et al., 2005; Wilson and Goodbred, 2015). The spatial variability of dissolved As is influenced by the hydro-stratigraphic settings shaped by these ancient (Aziz et al., 2008; Kazmierczak et al., 2022; Postma et al., 2007; Weinman et al., 2008) and recent fluvial processes (Stahl et al., 2016; Stute et al., 2007; Wallis et al., 2020). In their detailed study of the 25 km^2-sub-district of Araihazar in central Bangladesh, Weinman et al. (2008) reported that the dissolved As concentrations are largely influenced by the grain size, thickness, and distribution of fine-grained sediments overlying the buried sandy aquifers in Bangladesh. They demonstrated that the dissolved As concentrations were generally lower in areas where aquifer sands are exposed at or near the surface, but higher beneath or adjacent to thicker layers of find-grained deposits. Groundwater modeling (Desbarats et al., 2014; Mozumder et al., 2020) and tritium–helium age-dating (Stute et al., 2007) demonstrated orders of magnitude differences in travel times from ground surface to the depth of 20 to 30 m. This is the depth interval in which the highest dissolved As concentrations typically occur within shallow aquifers. Empirical studies in Araihazar found that shallow unconfined aquifers have average residence times of months to years, whereas clay or silt-capped aquifers typically have residence times of tens to hundreds of years (Aziz et al., 2008; Stute et al., 2007). Furthermore, shallow aquifers underlying floodplains which are annually inundated by river water have some of the highest As concentrations (Connolly et al., 2022). The physical or chemical processes that are initiated or prevented by certain types of surface lithology which impact As mobilization are still poorly understood.

The aforementioned observed spatial associations between shallow aquifer As concentrations and find-capped aquifers, including annually flooded floodplains, could be explained by: i) kinetically limited buildup of As concentrations in porewaters interacting with the longer physical travel times through clay and silt layers; ii) a finite amount of easily mobilizable As on sediments which is rapidly flushed from sands, but flushed slowly from clays and silts (van Geen et al., 2008); iii) reductants diffusing from clay layers which release As from aquifer sands by reduction of Fe(III)-oxides (Mihajlov et al., 2020); or iv) freshly deposited riverine sediments with abundant and easily mobilizable DOC which acts as the reductant for Fe(III)-oxides (Polizzotto et al., 2008). These mechanisms may not operate exclusively. Arsenic may be released in some places by a kinetically-governed slow process, such as silicate weathering, equilibrium-governed desorption or competitive desorption by phosphate, or have fast kinetics that are limited only by the supply of reactants as is the case for pyrite weathering in mountainous regions with high rates of physical weathering (Bufe et al., 2021).

The rate of microbially-mediated reductive dissolution of Fe(III)-oxides is limited by the availability and lability of DOC (Mailloux et al., 2013; Stopelli et al., 2021). In such settings where Fe(III)-oxides are the main pool of dissolved As to the aquifer, under anoxic conditions, Fe(III)-reducing bacteria utilize labile DOC as electron donors (ED) whereas Fe(III)-oxides act as electron acceptors (EA) (Islam et al., 2004; Postma et al., 2010). This dissimilatory reductive dissolution of Fe (III)-oxides mobilizes adsorbed As into pore-waters. The reduction of Fe (III)-oxides is therefore coupled to DOC oxidation/mineralization, which generates dissolved inorganic carbon (DIC) as a product. In this way, the cycling of As and iron (Fe) is closely related to the reactivity and availability of DOC in many aquifers.

Within the hyporheic zone (HZ) along the banks of a river with a transiently fluctuating stage, dissolved oxygen (DO) and nitrate (NO_3^-) are driven into the riverbank thereby regulating the redox state of the HZ (Kaufman et al., 2017; Musial et al., 2016). Observations and modeling performed along banks of the Meghna River in Bangladesh indicated that semi-diurnal fluctuations in river stage driven by ocean tides drive a dynamic mixing zone of oxidizing surface water and reducing groundwater within the HZ (Berube et al., 2018; Datta et al., 2009; Huang et al., 2022; Jung et al., 2015). This mixing between two chemically-distinct water bodies promotes the precipitation of Fe(III)-oxides within the HZ which removes dissolved As from the discharging groundwater. This process is referred to herein as a Natural Reactive Barrier (NRB) (Berube et al., 2018; Johnston et al., 2015; Jung et al., 2015; Mackay et al., 2014; Nagorski and Moore, 1999). An NRB can be thought of as the reconstitution of the products of reductive dissolution of Fe(III)-oxides which had previously occurred upgradient in the aquifer (Jewell et al., 2023).

The prevalence and persistence of NRBs though time and space are uncertain. The Fe and As bound within NRBs may not be stable long-term owing to seasonal oscillations in riverbank redox conditions. Under anoxic conditions, the previously precipitated amorphous Fe(III)-oxides within the HZ can become a significant source of aqueous As and Fe (Huang et al., 2022; Parsons et al., 2013). This is because amorphous Fe(III)-oxides have surface areas (~600 m^2/g) that are an order of magnitude higher than more crystalline Fe(III)-oxides and possess positively and negatively charged sorption sites (Dixit and Hering, 2003; Jung et al., 2012; Parsons et al., 2013). Therefore, the chemical stability of these Fe(III)-oxides and that of their bond to As impact the conditions under which an NRB functions as a sink or source of aqueous As and Fe. For example, laboratory experiments by Parsons et al. (2013) revealed that redox oscillations in calcareous floodplain sediments regulate As mobility via Fe(III)-oxide recrystallization. In their experiments, As was mobilized under reducing conditions, but repetitive cycling between oxidizing and reducing conditions had the net effect of immobilizing dissolved As.

Berube et al. (2018) and Jewell et al. (2023) demonstrated active accumulation of As in the HZ in two sites in the riverbank aquifers along the tidal Meghna River during the dry season. Along the same reach of the Meghna River widespread high concentrations of Fe(III)-oxides and As were observed within the shallow riverbank sediments (<1 m) (i.e., 17–599 mg/kg in Berube et al., 2018; 100–20,000 mg/kg in Datta et al., 2009). One study observed such deposits up to 5 m deep (1–709 mg/kg in Jung et al., 2015). We hypothesize two ways these deposits of high Fe (III)-oxides with As may form. The first hypothesis is that they are formed by advected groundwater carrying the reactants Fe and As towards the river and then mixing through advection and dispersion with the oxygenated river water within sandy, permeable sediments. The second hypothesis is that fine sediments high in solid-phase Fe and As concentrations are selectively deposited on the riverbanks by physical riverine and tidal sediment transport by receding floodwaters. Two of the aforementioned studies measured grain size (Berube et al., 2018; Jung et al., 2015) and found that the highest Fe(III)-oxide-As deposits were located in sandy material. This finding is consistent with the first hypothesis since silt and clays deposited along riverbanks discourage advective mixing with the river and therefore would not be an expected accumulation site for Fe(III)-oxides up to 1 m deep into the sediment (Jung et al., 2015). Further support for the first hypothesis came from a study by Huang et al., 2022 who reported that the amount of sedimentary As accumulated at three sites along an 13 km reach of the Meghna River in central Bangladesh approximately matches the calculated mass fluxes of dissolved As in groundwater towards the river over a period of 200 years during which the river's course has been stable. The

first hypothesis requires strong advective and dispersive mixing between river water and discharging groundwater. Under such conditions, sedimentary As should be associated with Fe(III)-oxides in sand. The second hypothesis is supported by the fact that silts and clays are chemically weathered and have substantial, charged surface areas which can also be enriched in solid-phase As. Furthermore, seasonally flooding, and especially tidal, rivers develop thick overbank mud deposits of fine material (Wilson et al., 2017; Wilson and Goodbred, 2015). These are very different processes. Once formed, each of these types of deposits could represent a potential source of dissolved As to shallow aquifers at a later time, but the As would be mobilized in different ways.

Given the diversity of physical and (bio)geochemical processes that drive toxic As concentrations across shallow aquifers in the GBM delta, it is important to study the chemical reactions that dissolved As undergoes at the end of the shallow aquifer flow path at a wide range of sites and along multiple rivers with contrasting present-day flow regimes and geologic architecture. Although the impact of the NRB on As mobility along the banks of the Meghna River has been demonstrated in several studies, little is known about how surficial lithology more generally influences mobilization or immobilization of As in riverbanks along tidal rivers. Jung et al. (2015) hypothesized that riverbank aquifers with silty-clay surficial deposits are less likely to form an NRB due to limited mixing between river water and groundwater. However, recent studies have demonstrated that silt and clay deposits are important sources of dissolved As in underlying or overlying aquifers (Erban et al., 2013; Mihajlov et al., 2020; Planer-Friedrich et al., 2012; Polizzotto et al., 2008; Smith et al., 2018). Therefore, the processes whereby riverbank surficial lithology regulates the chemical and mineralogical association of As need to be tested along other tidal rivers and across the riverine to tidal continuum. This study enhances understanding of conditions leading to mobilization and immobilization of As and offers new insights into the dynamics of As and Fe cycles in the shallow riverbank aquifers.

2. Materials and methods

2.1. Study area and site description

2.1.1. Background of the Hooghly River

The two riverbank study areas are located approximately 100 km apart along the Hooghly River. The Hooghly River is a distributary of the Ganges River, in the state of West Bengal in India (Fig. 1). The Hooghly River experiences semi-diurnal tidal and seasonal fluctuations similar to the Meghna River in Bangladesh (Chugh, 1961). Theses tides extend upstream for approximately 300 km upstream from the river estuary in the Bay of Bengal (Chugh, 1961; Deb and Chakraborty, 2015, 2013). At Kolkata the river experiences a mean spring tide of 5.1 m (ranging from 4.6 to 5.6 m), and a mean neap tide of 3.0 m (ranging from 2.4 to 3.6 m), for a mean neap-spring tide amplitude of 2.1 m (Deb and Chakraborty, 2015, 2013). The shallow Holocene aquifers (<60 m below ground level, bgl) along the banks of Hooghly River in West Bengal are typically unconfined and recharged annually by the monsoonal rainfall. The river tends to be losing during the monsoon season and gaining during the dry season (Kanuri et al., 2019; Mukherjee et al., 2018, 2007; Sankar et al., 2014). The Hooghly River is characterized by its shallow riverbank aquifers containing As-rich sediment, which had eroded from the Himalayas and were deposited throughout the late Pleistocene and Holocene (Bhowmick et al., 2013; McArthur et al., 2018, 2010, 2004). Shallow aquifers along the Hooghly riverbanks contain elevated

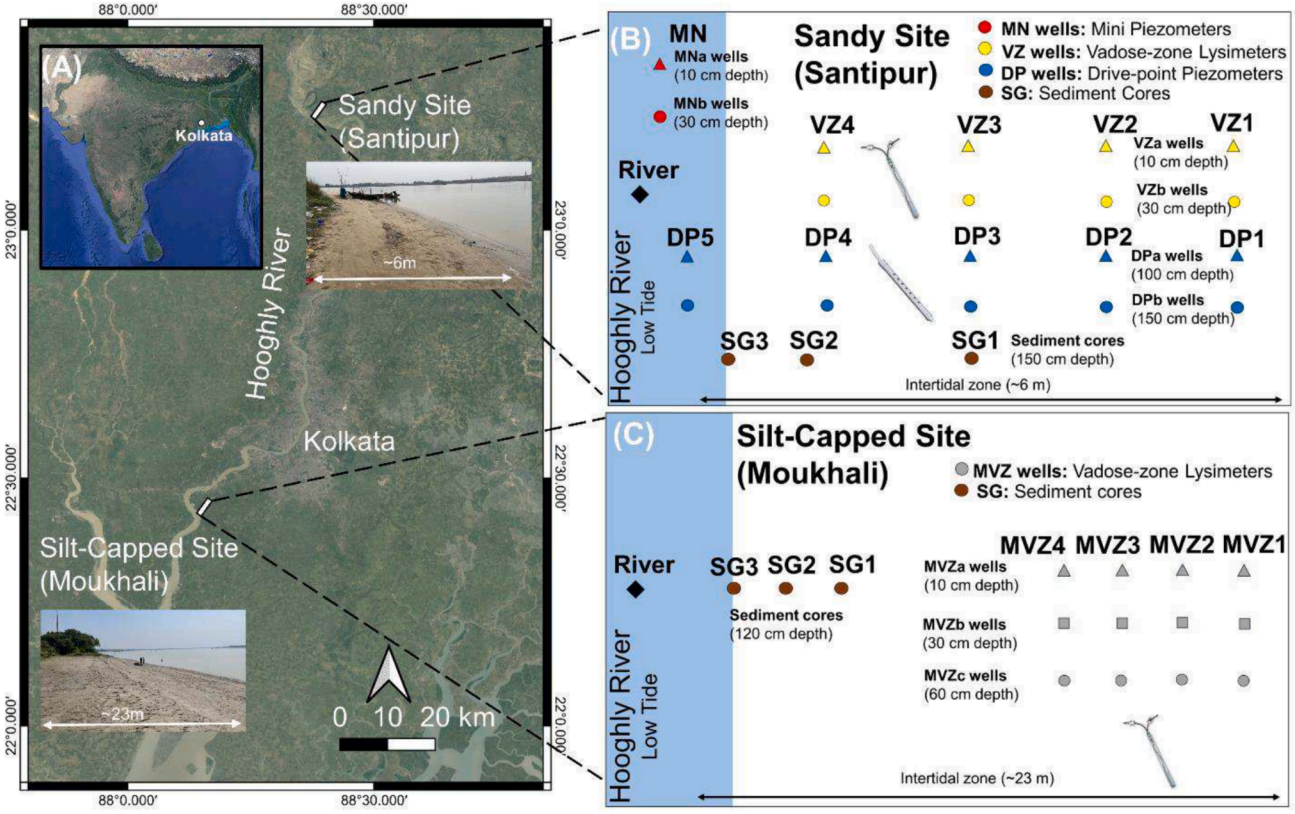

Fig. 1. Site description and configuration of sampling wells and sedimentary cores. (A) Location of the two study sites on the eastern bank of the Hooghly River in India. (B) Spatial location of sampling wells and sedimentary cores at the Sandy Site. The Sandy Site is located approximately 80 km north of the city of Kolkata, close to the town called Santipur (SG). This site is located at a highly permeable sandy riverbank. (C) Spatial location of sampling wells and sedimentary cores at the Silt-Capped Site. The Silt-Capped Site is located approximately 20 km south of the Kolkata, close to the town called Moukhali (MK). This site is located at a silt and/or clay-capped riverbank aquifer. All wells were numbered in descending order away from the river. For example, the DP well that is furthest from the river and has the shallowest depth is referred to as "DP1a".

concentrations of dissolved As and Fe, averaging 481 μg/L and 5.2 mg/L, respectively (Bhowmick et al., 2013; Chakraborti et al., 2009; McArthur et al., 2018, 2010, 2004).

In recent decades, human interventions have disrupted the hydro-geomorphological regime of the Hooghly River, with an example being the construction of the Farakka Barrage by the Indian government in 1975. This barrage, built across the main channel of the Ganges River in Murshidabad district in West Bengal, was initially designed to divert and regulate the supply of dry season freshwater flows from the upstream Ganges River to the downstream delta region and to improve the navigability of the Bhagirathi-Hooghly river system (Islam and Guchhait, 2020; Paszkowski et al., 2021). This modification of the hydro-geomorphological environment substantially changed the hydrology and the geomorphic balances in the south-west Ganges-dependent regions (Islam and Guchhait, 2020, 2017; Mirza, 1997; Murshed et al., 2019; Paszkowski et al., 2021). Islam and Guchhait, (2017) reported that the banks of Bhagirathi-Hooghly River have experienced increased erosion rates and a more pronounced channel straightening since the construction of the barrage in 1975. The average monsoonal discharge of the Farackka barrage down the Hooghly River is 3000 ± 1500 m^3/s, with the maximum discharge of up to 4200 m^3/s during September and a minimum of 900 m^3/s during May.

2.1.2. Description of the two riverbank study sites

We developed two new riverbank sites along the east bank of Hooghly River in the state of West Bengal in India (Fig. 1). Key physical characteristics were sought. First, we sought riverbanks that were not disturbed by any human-made structures, which was challenging given that most riverbanks in the Kolkata area had been developed as ghats, ports, or other human-made structures. Second, we sought riverbanks that span the entire intertidal zone, experiencing submersion twice a day under the influence of semi-diurnal tides. Third, we chose the field sites based on their easy accessibility and proximity to the city. Lastly, the field sites were chosen for their contrasting surficial lithologies, determined by visual inspection of initial sedimentary cores. The large distance between the sites means that the tidal amplitudes are higher at the downstream site. Silt-capped banks increasingly dominate tidal rivers with proximity to the coast owing to the backwater effect (Wilson et al., 2017). Therefore, the upstream site is characterized by shallow sand aquifer and the downstream site has a silt-capped shallow aquifer. This is consistent with findings from previous regional studies conducted in West Bengal, which observed that the percentage of sand in the sediment gradually decreased downstream, leading to higher clay content in the sediment (Mondal et al., 2018, 2020; Sarkar et al., 2017; Trifuoggi et al., 2022). Trifuoggi et al. (2022) reported that sediments from a site near our upstream sand site contained average of 19.5 % sand, 30.8 % silt, and 49.7 % clay, whereas a site near our downstream silt-capped site contained 14.9 % sand, 33.4 % silt, and 51.6 % clay.

The two sites were chosen to test the two hypotheses previously presented. The first site, chosen to test the first hypothesis, is located approximately 80 km north of the city of Kolkata, close to the town called Santipur (SG) (Fig. 1A). The site is located at the eastern bank of the Hooghly River and has highly permeable sandy surficial deposits, herein referred to as the Sandy Site. This site has similar geology to several previously characterized sites previously along the banks of the Meghna River (Berube et al., 2018; Jung et al., 2015). The sandy riverbank spans approximately 6 m from the river edge. The riverbank spans the entire intertidal zone, where it is submerged twice a day by semi-diurnal tides. Satellite imagery analysis and erosion volume estimation demonstrated that the banks at this site experienced high levels of erosion (estimated range 10.8 to 21.9 Mm^3) since 1990 (Mukhopadhyay et al., 2023).

The second site, chosen to test the second hypothesis, is located approximately 20 km south of the city of Kolkata, close to the town called Moukhali (MK) (Fig. 1A). This site has a surficial silt and/or clay-capped riverbank aquifer at the eastern bank of the Hooghly River, herein referred to as the Silt-Capped Site. This site is hypothesized to limit the mixing of Fe(II)-rich groundwater and oxygen-rich river water along the parafluvial zone in the riverbank. Therefore, it is hypothesized that due to limited source of riverine oxygen, an NRB would not form at the end of the flow path at this site. This site experiences greater tidal fluctuations than the Sandy Site with strong backwater effects. Thus, the site accumulates new silt deposits. The riverbank spans approximately 23 m from the river edge and is submerged twice a day. The estimated erosion volumes of riverbank sediment at the banks at this site since 1990 were lower (estimate range 1.8 to 5.3 Mm^3) than the Sandy Site (Mukhopadhyay et al., 2023). The surficial lithologies of the sites were determined by visual inspection of sedimentary cores.

2.1.3. Groundwater well installation and sedimentary core collection

At the Sandy Site, twenty-one drive-point piezometers and vadose-zone lysimeters were installed across a 6 m-long transect oriented orthogonal to the river shoreline (Fig. 1B). The transect was composed of three different types of wells: i) ten drive-point piezometers were installed to collect depth-specific groundwater samples from below the water table to analyze chemical composition in the riverbank aquifer to depths of 1 and 1.5 m bgl. These wells were composed of a stainless-steel drive-point piezometer head with 15 cm screen (Model 615, Solinst Canada Ltd, Georgetown, ON, Canada) and a 16 mm outer diameter stainless-steel pipe. These wells are referred to hereafter as the DP wells; ii) eight 22 mm outer diameter vadose-zone lysimeters (SSAT, Irrometer Company Inc., Riverside, CA) were installed across the intertidal zone to sample the porewater above the dynamically fluctuating water table in the vadose-zone. These wells are referred to hereafter as the VZ wells; and iii) two mini-piezometers were installed in the riverbed, located several meters from the river shoreline to sample upwelling groundwater before it discharges to the river. These wells are referred to hereafter as the MN wells. Lastly, one river water sample was collected at each site 30 cm below the water surface 5 m from the riverbank.

Three 1.2 m long sediment cores were collected along a transect orthogonal to the river from the low tide shoreline to 2.5 m inland. The cores were collected using a direct push sediment probe (Sediment Sampler, AMS Inc., American Fall, ID) with a slide hammer loaded with clear plastic liners (2.5 cm diameter and 60 cm length). These cores were collected to measure sediment chemistry generally, and to examine associations between Fe and As and mineral phases.

At the Silt-Capped Site, a total of 12 vadose-zone lysimeters were installed across an approximately 23 m-long transect oriented orthogonal to the river shoreline (Fig. 1C). Vadose-zone lysimeters were installed to sample porewaters at depths of 10, 30, 60 cm bgl. These wells are referred to hereafter as the MVZ wells. Three 1.2 m length sediment cores were collected from the low tide shoreline to 3.5 m inland. Grain sizes of all sediment cores were estimated on-site by hand observation.

2.2. Aqueous phase chemistry analysis

2.2.1. On-site aqueous chemistry measurements

Each DP well was pumped until temperature, pH, specific conductance (SC) and Oxidative-Reductive Potential (ORP) stabilized. The DP wells were pumped with a peristaltic pump (Model 410, Solinst Canada Ltd., Georgetown, ON, Canada) with the manufacturer's low-flow adaptor and size 15 Masterflex tubing. The target flow rate was 50 mL/min. Each VZ and MVZ well was depressurized with a bicycle pump. Equipped with a permeable ceramic cup on the end, these lysimeters absorb vadose-zone porewater from the surrounding soil as they are placed under vacuum. Redox-sensitive groundwater parameters, DO, NO_3^-, ammonium (NH_4), sulfide (H_2S), manganese Mn^{2+}, and Fe^{2+} were measured on-site using colorimetric tests with a portable spectrophotometer (V-2000, CHEMetrics Inc., Midland, VA). Approximate concentrations of dissolved total As were measured on-site using a colorimetric arsenic test kit with an accuracy of ±18 ppb (Econo-Quick

arsenic test kit, Industrial Test Systems Inc., Rock Hill, SC).

The larger tidal fluctuations at the Silt-Capped Site, limited access to the riverbank, and the low permeability of the silt meant that there was insufficient time to sample the porewaters. Therefore, on-site aqueous chemistry measurements were solely conducted at the Sandy Site. However, the porewater samples for laboratory aqueous chemistry measurements were collected both at the Sandy site and the Silt-Capped site.

2.2.2. Laboratory aqueous chemistry measurements

Thirty-one water samples were collected at the Sandy Site and the Silt-Capped Site to perform laboratory aqueous chemistry measurements. All water samples to be analyzed by laboratory instruments were filtered on-site through a 0.45 μm nitrocellulose syringe filter (Millipore Millex – HP, Merck KGaA, Darmstadt, Germany) using a plastic syringe into acid-cleaned 20 mL High Density Polyethylene (HDPE) vials that were pre-rinsed at least three times with the sample water. Major cations (Na^+, NH_4^+, K^+, Mg^{2+}, Ca^{2+}) and anions (Cl^-, Br^-, SO_4^{2-}, F^-, NO_3^-, and NO_2^-) were analyzed using ion chromatography (IC) (Thermo Dionex Integrion, Thermo Fisher Scientific, Waltham, MA). The cation and anion samples were stored in a refrigerator at 4 °C and analyzed by IC at the Texas A&M University (TAMU) within 4 weeks of sampling.

Water samples for DOC analysis were filtered through 0.7 μm diameter ashed GF/F syringe filters (Whatman, Cytiva, Marlborough, MA) and stored in 40 mL amber glass vials that were pre-loaded with 20 μL of 12 M Optima grade HCl. The DOC samples were stored in a refrigerator at 4 °C (Fellman et al., 2008) and analyzed as non-purgeable organic carbon (NPOC) by a Shimandzu TOC-VCSH at the Hazen Research lab within 2 weeks of sampling (Hazen Research Inc., Golden, CO), following United States Environmental Protection Agency (USEPA) method 415.1 (Potter and Wimsatt, 2005). The alkalinity of groundwater samples was measured on the same day of sampling following a modified Gran titration method (Appelo and Postma, 2005; Gran, 1952). The 0.0145 M HCl titrant was used to perform titrations on the water samples, with an approximately volume of 15 mL.

2.3. Sediment core analyses

The collected sediment cores were immediately sealed in-situ using a fitted rubber cap and electrical tape to discourage oxygen diffusion. The cores were stored at −10 °C in a freezer and analyzed within 4 weeks of sampling. The sediment cores were subdivided into 5 to 10 segments of 10 to 15 cm in length to analyze for the depth-specific sedimentary chemistry of the two field sites (Sandy site, n = 23; Silt-Capped Site, n = 19).

2.3.1. Elemental and mineralogical characteristics of sediments

The bulk elemental compositions of the sediment samples were determined using a hand-held X-ray fluorescence (XRF) spectrometer (Niton XL3t 500 GOLDD, Thermo Scientific, Waltham, MA). All the sediment from each segment was homogenized, placed in a trimmed paper cup with diameter of 2.2 cm, and covered with clear polyethylene wrap. Data collection involved a 180-second measurement time on each sediment sample (60 s for the main filter, 60 s for the low filter, and 60 s for the light filter) at a maximum voltage of 40 kV. Two standard reference materials, NIST 2709a and CCRMP Till-4, were measured, indicating an average difference of 8.1 % from the certified As concentrations. This falls well within the acceptable error range of 20 % for the hand-held XRF.

To estimate the redox state and abundance of sedimentary Fe, the diffuse reflectance spectrums of the sediment samples were measured using a spectrophotometer (CM-600d, Minolta Corp., Tokyo, Japan) following a previously established method that is summarized below (Horneman et al., 2004). The sediment samples were prepared in a paper cup covered with clear polyethylene wrap (n = 42). The measurements were recorded in relation to a $BaSO_4$ standard, using a D65 illuminant with the instrument's observer angle set to 10°. Two readings were taken for each sample. Each reading is an automated average of 5 measurements. To determine the statistical differences between the riverbank types, a Mann-Whitney *U* test was performed using a significance value of $p = 0.05$ using JMP pro 17 software (JMP Statistical Discovery LLC, Cary, NC).

2.3.2. Sediment extractions

Sediment extractions using either deionized (DI) water or 1.2 N HCl were performed on the collected sediment samples from the two study sites (Sandy Site, n = 11; Silt-Capped Site, n = 11).

The water-extraction experiment was performed to determine the concentration of water-soluble constituents in the sediment samples. For each extraction, 1 g of sediment was placed in a 50 mL centrifuge tube containing 40 mL of DI water. The tubes were then placed on a shaker table to mix for 24 h at 75 rpm under oxic conditions at room temperature. After 24 h, the slurries were centrifuged, and the pH and SC of the supernatant were immediately measured. The supernatant was then filtered through a 0.45 μm syringe filter and separated into two separate aliquots for subsequent analyses (unacidified and 0.2 % v/v HNO_3 acidified).

A separate HCl-extraction experiment was performed to determine the concentrations of the constituents associated with reducible and amorphous Fe(III)-oxides. For each experiment, 1 g of sediment sample was placed in a 15 mL centrifuge tube containing 10 mL of 1.2 N HCl solution. The slurry was then placed in a 75 ± 5 °C hot water bath for one hour. After one hour, 0.5 mL of the supernatant was filtered through a 0.45 μm syringe filter and diluted by a factor of 100.

Major and trace elements of the extracts from the two leaching experiments were measured by Inductively Coupled Plasma Mass Spectrometry (ICP-MS) (Agilent 7850 ICP-MS, Santa Clara, CA, USA) following an internal analysis method at the Advanced Materials Research Centre (AMRC) at the Indian Institute of Technology, Mandi. The concentrations of Fe(II) in the HCl extracts were determined by the Ferrozine method at an absorbance of 562 nm using a single beam benchtop spectrophotometer. The HCl-extractable concentrations of Fe (III) in the sediment samples were calculated by subtracting the Fe(II) concentrations measured by the Ferrozine method and the total Fe concentrations in the HCl-extracts determined by ICP-MS.

2.4. Multivariate analysis and geochemical modeling

2.4.1. Principal Components analysis

To visualize the correlation structure of aqueous and sedimentary chemical parameters and thereby identify clusters of samples whose chemical properties differ from each other, the aqueous and sedimentary geochemistry data were analyzed by Principal Components Analysis (PCA) using JMP Pro 17 and *Scikit.learn*, an open access Python machine learning library. Principal Components Analysis reduces the number of variables into principal components (PCs). These PCs are ranked by the proportion of the total variance they describe in descending order. Principal Components Analysis was performed four times on the aqueous and sedimentary chemical parameters for both the Sandy Site and the Silt-Capped Site samples.

2.4.2. Calculating saturation indices and charge balance error

To determine the dominant geochemical processes along the flow path across the shallow riverbank aquifers by establishing the thermodynamic status of each mineral, saturation indices (SIs) were calculated for major prospective minerals, including Fe(III) oxide minerals, sulfate minerals, carbonate minerals, and evaporites. These were plotted spatially to visualize how SIs evolve along the flow-paths discharging to the river. Groundwater chemistry parameters, including temperature, pH, alkalinity, DO, NO_3^-, NH_4, H_2S, Mn^{2+}, Fe^{2+}, As, Na^+, NH_4^+, K^+, Mg^{2+}, Ca^2, Cl^-, Br^-, SO_4^{2-}, NO_3^-, and NO_2^-, were entered into PHREEQC Interactive software Version 3. The Wateq4f database was utilized in the

calculations. Two redox couples (O(0)/O(−2) and N(−3)/N(5)) were utilized to estimate the redox state or Eh of the porewaters. The model speciates redox-sensitive dissolved elements such as Fe and As according to the Eh. In the case of Fe, the oxidized species precipitates fully as Fe (III)-oxides. Therefore, modeled dissolved concentrations of redox-sensitive species may strongly differ from the observed concentrations and the SI values of minerals which contain redox-sensitive elements are highly sensitive to the value of Eh. Detailed descriptions of methods of the calculation of Charge Balance Error (CBE) can be found in the supplementary information (Text S1).

3. Results and discussion

3.1. Natural reactive barrier at the sandy site

At the Sandy Site (Fig. 1B), dissolved As and Fe concentrations consistently decreased along the groundwater flow path towards the Hooghly River (1000 to 0 μg/L and 10 to 0.1 mg/L, respectively) (Fig. 2A and B). River water samples contained low concentrations of dissolved As and Fe^{2+} (0 μg/L and 0.1 mg/L) (Fig. 2A and B). Nitrate (NO_3^-) concentrations decreased towards the river (4.3 to 0.7 mg/L) (Fig. 2C), however, dissolved oxygen (DO) concentrations were consistently high in the riverbank, ranging from 5.1 to 8.0 mg/L, for all wells and lysimeters except for DP3b well, located 1.5 m from the low tide river edge (Fig. 2D). Well DP3b contained only 0.8 mg/L DO. This one exception notwithstanding, such high DO concentrations in a riverbank were not previously observed in any of the study sites in which porewater chemistry has been observed along the Meghna River (Berube et al., 2018; Jewell et al., 2023; Jung et al., 2012, 2015; Kwak et al., in press). Dissolved organic carbon (DOC) concentrations decreased towards the river (2.1 to 1.3 mg/L) (Fig. 2E). Dissolved inorganic carbon (DIC) concentrations, measured as alkalinity, were highest proximate to the river (185.9 to 952.6 mg/L) (Fig. 2F). If all the alkalinity is assumed to be from HCO_3^-, the concentrations of DIC range from 3 to 11 mmol. In contrast, only 0.02 mmol of carbon appears in DOC in the porewaters. Therefore, the observed high DIC concentrations cannot be generated from oxidation of DOC in porewaters across the flow path towards the river, but rather through decomposition of sedimentary organic carbon (SOC) (Aftabtalab et al., 2022; Gao et al., 2019; Lau et al., 2015; Schittich et al., 2018).

Porewater temperatures decreased towards the river (36 to 32 °C) (Fig. 2G). The higher temperature of the porewaters here (32 to 36 °C) compared to shallow aquifers in the region (24 to 27 °C) (Sankar et al., 2014) suggests that the proximity of water table to ground surface drives porewater temperatures higher as the mean daily temperature during the month of May is ~34 °C in Kolkata (Khan et al., 2015). Then, the decrease in temperature in the riverbank with proximity to the river is evidence of mixing with the cooler river water. The river has an average temperature of 30 °C this time of year (Kanuri et al., 2019).

The pH decreased with proximity to the river (7.7 to 7.0), whereas SC increased (391 to 1320 μS/cm) (Fig. 2H and 2I). The decrease in pH and increase in SC levels are chiefly caused by the aerobic respiration of SOC, which generates carbonic acid (H_2CO_3) which dissociates to HCO_3^- thereby increasing acidity and introducing the main anion. Spatial distributions of concentrations of major cations (Na^+, NH^{4+}, K^+, Mg^{2+}, Ca^{2+}) and anions (Cl^-, Br^-, SO_4^{2-}, NO_3^-, NO_2^-, and HCO_3^-) across the riverbank aquifer at the Sandy Site are presented in the supplementary information (Figs. S2-S3, Fig. S6, Text S2).

An actively growing NRB would manifest as an active sink for dissolved As and Fe within the HZ of riverbanks in gaining river systems (Berube et al., 2018; Datta et al., 2009; Huang et al., 2022; Jung et al., 2015). An active sink can be demonstrated by observing decreasing concentrations of As and Fe towards the river, after accounting for dilution with river water. At the Sandy Site, dissolved As and Fe^{2+} are removed from solution in the bidirectional mixing zone between discharging groundwater and the river. Products of aerobic respiration of SOC are generated at the same time. These results strongly suggest that an NRB is present and acting as a sink for both dissolved As and Fe at the end of the flow path at the Sandy Site with the abundant oxygen oxidizing both the SOC and the Fe^{2+} arriving from the aquifer. Such a highly oxygenated riverbank that is acting as an active sink of As and Fe has not previously been documented in the Bengal Basin to the authors' knowledge.

In the PC1 vs. PC2 loadings plot (Fig. S1), dissolved As and Fe^{2+}

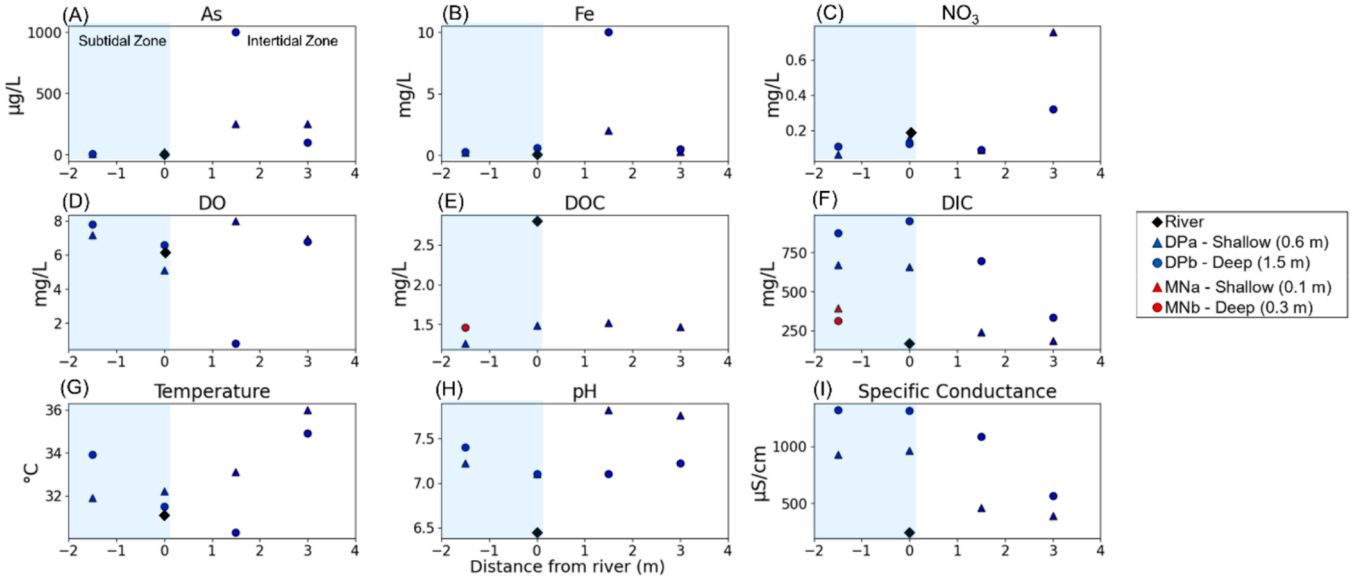

Fig. 2. Porewater chemistry profiles across the riverbank at the Sandy Site. Redox-sensitive elements As, Fe^{2+}, NO_3^-, and DO (A-D), dissolved carbon species (E-F), and field groundwater parameters (G-I) were plotted. Blue triangles and blue circles represent shallow (0.6 m) and deep (1.5 m) DP wells (drive-point piezometers), respectively. Red triangles and red circles represent shallow (0.1 m) and deep (0.3 m) MN wells (mini-piezometers), respectively. The black diamond represents the river water. The temperature and DO of the river are from Kanuri et al., 2019. The light blue box represents the stage of the Hooghly River at lowest tide (subtidal zone). The x axis describes the distance of each well from the dry season river shoreline during low, neap tide. (For interpretation of the references to colour in this figure legend, the reader is referred to the web version of this article.)

closely grouped. The loading vectors of As and Fe^{2+} plotted in the opposite quadrant to other redox-sensitive parameters such as DO and NH_4^+, which are the product of aerobic degradation of organic carbon. Thus, there is a strong negative correlation between As, Fe^{2+}, and DO, NH_4^+ across the riverbank. In the DP well that contained the highest concentrations of dissolved Fe^{2+} (~10 mg/L), the DO concentrations were the lowest (~0 mg/L). The wells with low concentrations of dissolved Fe (~0.1 mg/L) contained high DO concentrations (~8 mg/L) (Fig. 2B and D). The patterns in the multivariate data further support the contention that active precipitation of Fe(III) oxide minerals is a sink for dissolved As and Fe^{2+} at the Sandy Site. Studies published by Bhowmick et al. (2013) on the eastern bank of the Hooghly River in the area describe shallow aquifer As and Fe^{2+} concentrations that range from 164 to 798 μg/L and 2.8 to 7.6 mg/L, respectively. Thus, the similarly high dissolved As and Fe^{2+} concentrations in the intertidal zone 2–4 m away from the river edge are consistent with the notion of advected shallow groundwater carrying these reactants into the HZ.

The presence of abundant DO throughout the sandy riverbank leaves little doubt that this high energy EA drives oxidation of OC and dissolved Fe^{2+} within the aquifer system. This role of DO as the primary EA is a characteristic not previously identified in study sites along other riverbanks characterized in Asian deltas with shallow reducing aquifers. In these riverbanks, concentrations of DO and NO_3^- in porewater samples were always scarce (<1 mg/L) (Berube et al., 2018; Datta et al., 2009; Jewell et al., 2023; Jung et al., 2015; Kwak et al., in press; Larsen et al., 2008; Polizzotto et al., 2008; Postma et al., 2007). At their study site along the eastern bank of Meghna River during the dry season when tides exert a strong influence on river stage, Berube et al. (2018) observed that, despite the presence of high concentrations of solid-phase Fe(III)-oxides and net removal of As at the end of the flow path, a net positive flux of dissolved Fe^{2+} was still being released to porewaters in this zone. At another Meghna riverbank located 7 km upstream from the aforementioned one, Jewell et al. (2023) observed the same phenomenon of concurrent removal of As and release of dissolved Fe at the end of the flow path within a bidirectional mixing zone with the river. These two studies agreed that reductive dissolution of Fe(III)-oxides may occur concurrently with the sorption of dissolved As onto the remaining Fe (III)-oxides yet to undergo reduction. Jewell et al. (2023) suggested that this net removal of As in the face of reduction of some Fe(III)-oxides could be explained by the ambient chemistry produced by organic matter oxidation and silicate weathering within the floodplain, which produces abundant DIC, phosphate and silica. Laboratory studies demonstrated that these solutes in particular encourage the entrainment of As into stable crystalline forms of Fe(III)-oxides such as ferrihydrite and goethite (Senn et al., 2018). In contrast to these other sites where oxygen was scarce, along the riverbank of the Sandy Site in this study, both dissolved As and Fe^{2+} are actively removed from the porewaters, indicating that nearly all of the dissolved Fe^{2+} is actively being oxidized and precipitated within the riverbank aquifer.

Saturation indices for Fe(III)-oxide, carbonate, sulfate, and evaporite minerals were calculated to evaluate mineral solubility along the flow path across the Sandy Site's riverbank (Fig. 3). Iron oxide minerals were consistently supersaturated across the riverbank (Fig. 3A–C). Saturation indices for amorphous Fe(III)-oxides ranged approximately from 1.8 to 3, while those for goethite ranged approximately from 6 to 8 (Fig. 3A and B). Additionally, magnetite had SIs ranging from 15 to 22 (Fig. 3C). Calcite was near equilibrium (0 to 1) and increased with proximity to the river (Fig. 3D). Siderite was slightly supersaturated (0.1 to 1.3) in the 1.5 m deep DP wells on the exposed riverbank, but undersaturated (−4.7 to −3.0) near the water table in the 0.6 m deep DP wells (Fig. 3E). Mackinawite was undersaturated (−3.9 to −3.3) in the 0.6 m deep DP wells (Fig. 3G). Conversely, these samples were undersaturated for gypsum and halite (−3.6 to −3.2 and −7.8 to −8.4, respectively) (Fig. 3F and I) but were supersaturated (22.5 to 25.2) for pyrite (Fig. 3H). Thus, the precipitation of Fe(III)-oxide minerals is supported by thermodynamics. These serve as trap for dissolved Fe^{2+} and As at the end of the flow path at the Sandy Site's riverbank (Fig. 1).

3.2. Major cations and anions in porewaters at Silt-Capped Site

As previously mentioned, due to limited access to the riverbank at the Silt-Capped Site, only IC analysis was conducted on the porewater

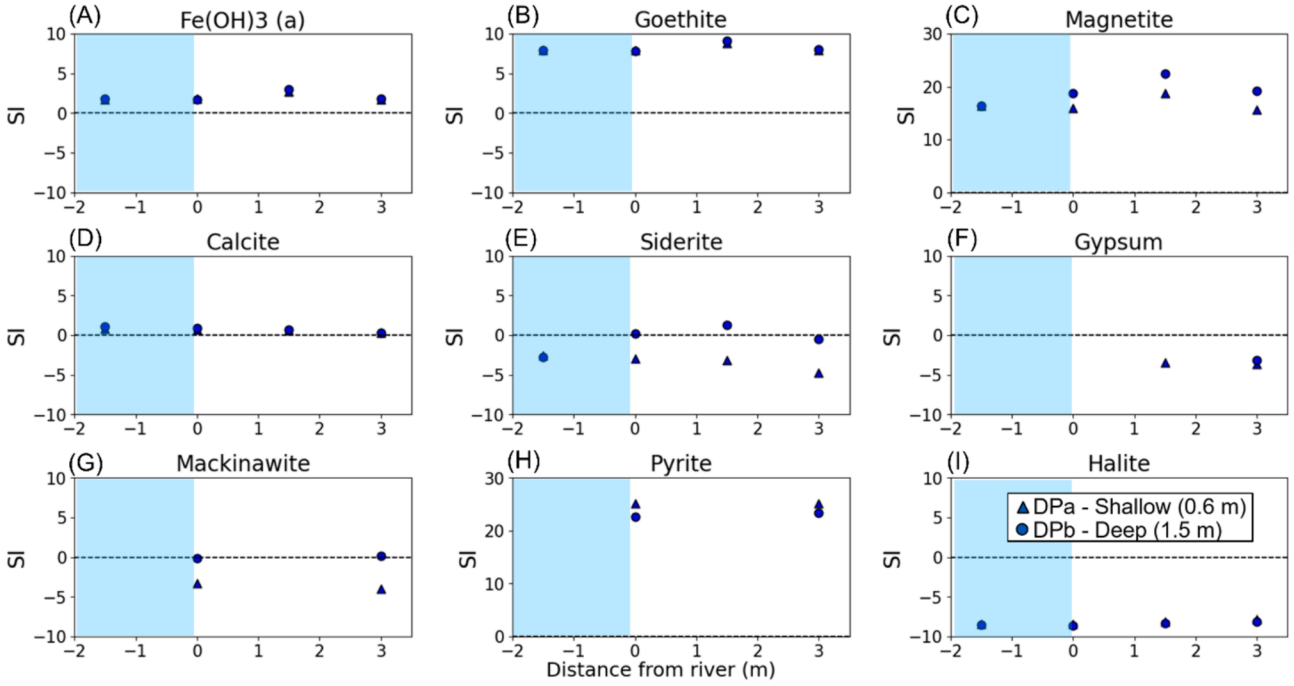

Fig. 3. Saturation indices of porewater samples from DP wells inferred from PHREEQC model using Wateq4f database. (A) amorphous Fe(III)-oxide (FeOOH), (B) goethite (α-FeOOH), (C) magnetite (Fe_3O_4), (D) calcite ($CaCO_3$), (E) siderite ($FeCO_3$), (F) gypsum ($CaSO_4{\cdot}2H_2O$), (G) mackinawite (FeS), (H) pyrite (FeS_2), and (I) halite (NaCl).

samples from the site. Spatial distributions of major cations (Na^+, NH^{4+}, K^+, Mg^{2+}, Ca^{2+}) and anions (Cl^-, Br^-, SO_4^{2-}, NO_3^-, NO_2^-, and HCO_3^-) across the vadose-zone at the Silt-Capped Site are presented in the supplementary information (Figs. S4–S6, Text S2).

3.3. Higher proportions of crystalline Fe(III)-oxides at the sandy site than the silt-capped site

A total of six sediment cores were collected from the two field sites, each subdivided into 5 to 10 segments with 10 cm to 15 cm lengths, to assess the depth-specific sedimentary chemistry along the riverbanks. Approximate grain size of the sediment at each site were estimated by hand observation. The Sandy Site riverbank had homogeneous medium sand, whereas the Silt-Capped Site riverbank had predominantly silt to silty-clay with intercalating fine sand (Table S2). The average concentrations of bulk sedimentary As and Fe, measured by a hand-held XRF differed between the two sites. At the Silt-Capped Site, the bulk As and Fe concentrations (9.0 ± 5.6 mg/kg and 18.5 ± 3.0 g/kg, respectively) were greater than those found at the Sandy Site (2.8 ± 1.3 mg/kg and 10.7 ± 4.0 g/kg, respectively) (Table. 1, Fig. 4). The concentrations and proportions (concentrations compared to bulk concentrations measured by XRF) in mobilizable phases, measured by DI water and HCl extractions also differed between the sites. Sediment cores from the Silt-Capped Site contained higher concentrations and proportions of mobilizable As and Fe compared to those obtained from the Sandy Site (Table. 1, Fig. 4). The Silt-Capped Site sediment contained 0.3 mg/kg of water-extractable As (4 % of the bulk As concentrations) and 2.3 mg/kg of HCl-extractable As (26 %), whereas the Sandy Site sediment contained 0.1 mg/kg of water-extractable As (1.8 %) and 0.7 mg/kg of HCl-extractable As (25 %). The Silt-Capped Site sediment contained 40.5 mg/kg of water-extractable Fe (0.2 % of the bulk Fe concentrations), 0.8 g/kg of HCl-extractable Fe(II) (4.3 %), and 7.0 g/kg of HCl-extractable Fe_{total} (37.5 %). The Sandy Site sediment contained 3.0 mg/kg of water-extractable Fe (0.03 %), 0.3 g/kg of HCl-extractable Fe(II) (2.6 %), and 2.9 g/kg of HCl-extractable Fe_{total} (26.9 %).

Differences in the redox state of sedimentary Fe between the Sandy Site and the Silt-Capped Site are further described by the diffuse reflectance measurements. The first transform derivative of diffuse reflectance measurements (ΔR) at 520 nm can be used to estimate the proportions of more crystalline Fe(III)-oxides, such as goethite or hematite, in sediments (Horneman et al., 2004). Despite the sand from the Sandy Site containing lower concentrations of bulk sedimentary Fe, it consistently had higher ΔR values at 520 nm (average 0.38) in comparison to silt from the Silt-Capped Site (average 0.17) (Fig. 5A). Previous observations have indicated an inverse correlation between the Fe (III) and Fe(II) in sediments (Horneman et al., 2004). This inverse correlation was the case for the Hooghly riverbank sediments, where the proportion of HCl-extractable Fe(II) displayed an inverse correlation with ΔR at 520 nm (R^2 = -0.65, p = 0.002) (Fig. 5B). Thus, the sand contains higher proportions of crystalline Fe(III)-oxides such as goethite or hematite than the silt.

In addition to the differences in bulk sedimentary As and Fe concentrations and their proportions in mobilizable phases between the Sandy Site and the Silt-Capped Site the relationship between solid-phase As and Fe concentrations differed drastically between the two sites. HCl-extractable As and Fe concentrations were correlated in the Sandy Site sediments (R^2 = 0.74, p = 0.001), whereas at the Silt-Capped Site, there was a weak negative relationship between As and Fe (R^2 = 0.40, p > 0.05) (Fig. 5C). In contrast, HCl-extractable Fe(II) and Al in the Silt-Capped Site were strongly related (R^2 = 0.91, p = 0.001), suggesting an association between Fe(II) and aluminosilicate clay minerals in the

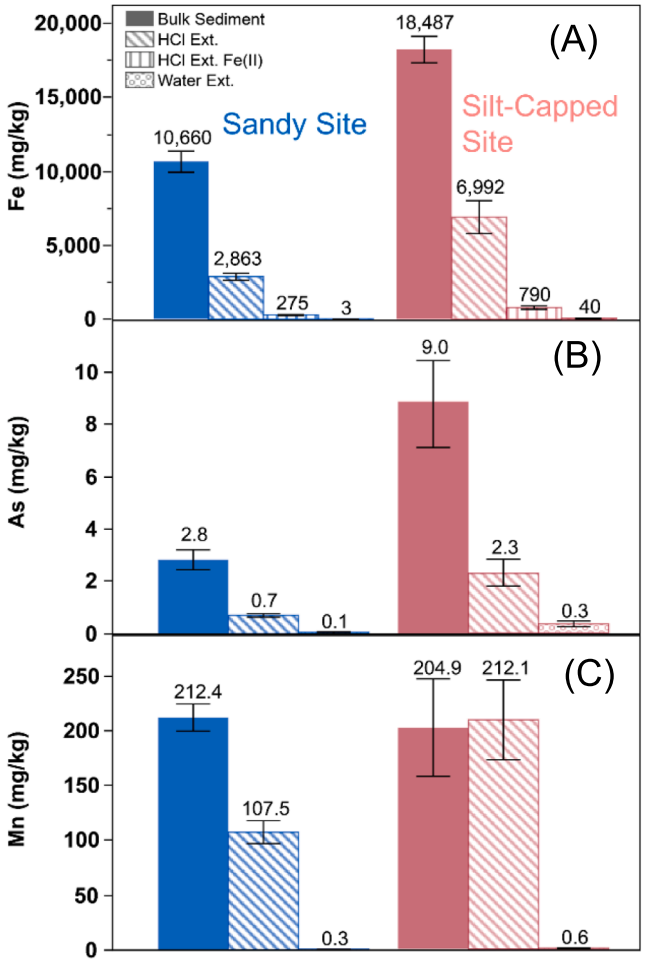

Fig. 4. Bulk sedimentary, HCl extractable, and water extractable concentrations of (A) Fe, (B) As, and (C) Mn. For visual comparison, the Sandy Site sediment samples are grouped on the left side of the plot in blue and the Silt-Capped Site sediment samples are grouped on the right side of the graph in red. (For interpretation of the references to colour in this figure legend, the reader is referred to the web version of this article.)

Table 1
Table showing the average measurements with standard deviation for the bulk solid-phase, water-extractable, and the HCl extractable parameters. The values in parentheses represent the minimum and maximum values measured for each parameter.

	Bulk Sediment				Water Extracts			HCl Extracts			
	Fe (g/kg)	As (mg/kg)	Mn (mg/kg)	ΔR 520 nm	Fe (mg/kg)	As (mg/kg)	Mn (mg/kg)	Fe (g/kg)	Fe(II) (g/kg)	As (mg/kg)	Mn (mg/kg)
Sand (n = 11)	10.7 ± 1.7 (8–16)	2.8 ± 1.3 (1–5)	212 ± 41 (150–280)	0.4 ± 0.1 (0.3–0.5)	3.0 ± 2.0 (1.1–6.5)	0.1 ± 0.1 (0–0.1)	0.3 ± 0.2 (0–1)	2.9 ± 0.8 (2–5)	0.3 ± 0.1 (0.2–0.5)	0.7 ± 0.2 (0.4–1.0)	107 ± 35 (76–195)
Silt (n = 11)	18.5 ± 3.0 (15–26)	9.0 ± 5.6 (5–23)	205 ± 150 (0–401)	0.2 ± 0.2 (0–0.4)	40.5 ± 60.0 (3–175)	0.3 ± 0.3 (0–1)	0.6 ± 0.8 (0–3)	7.0 ± 3.7 (2–15)	0.8 ± 0.4 (0.3–1.5)	2.3 ± 1.7 (1.0–6.4)	212 ± 122 (55–372)
MWW pvalue	**<0.001**	**<0.001**	0.948	**0.001**	**<0.001**	**<0.001**	0.793	**0.003**	**<0.001**	**<0.001**	0.149

Bold text denotes statistical differences (p < 0.05) between the silt and sand based on a non-parametric Mann-Whitney-Wilcoxon Test.

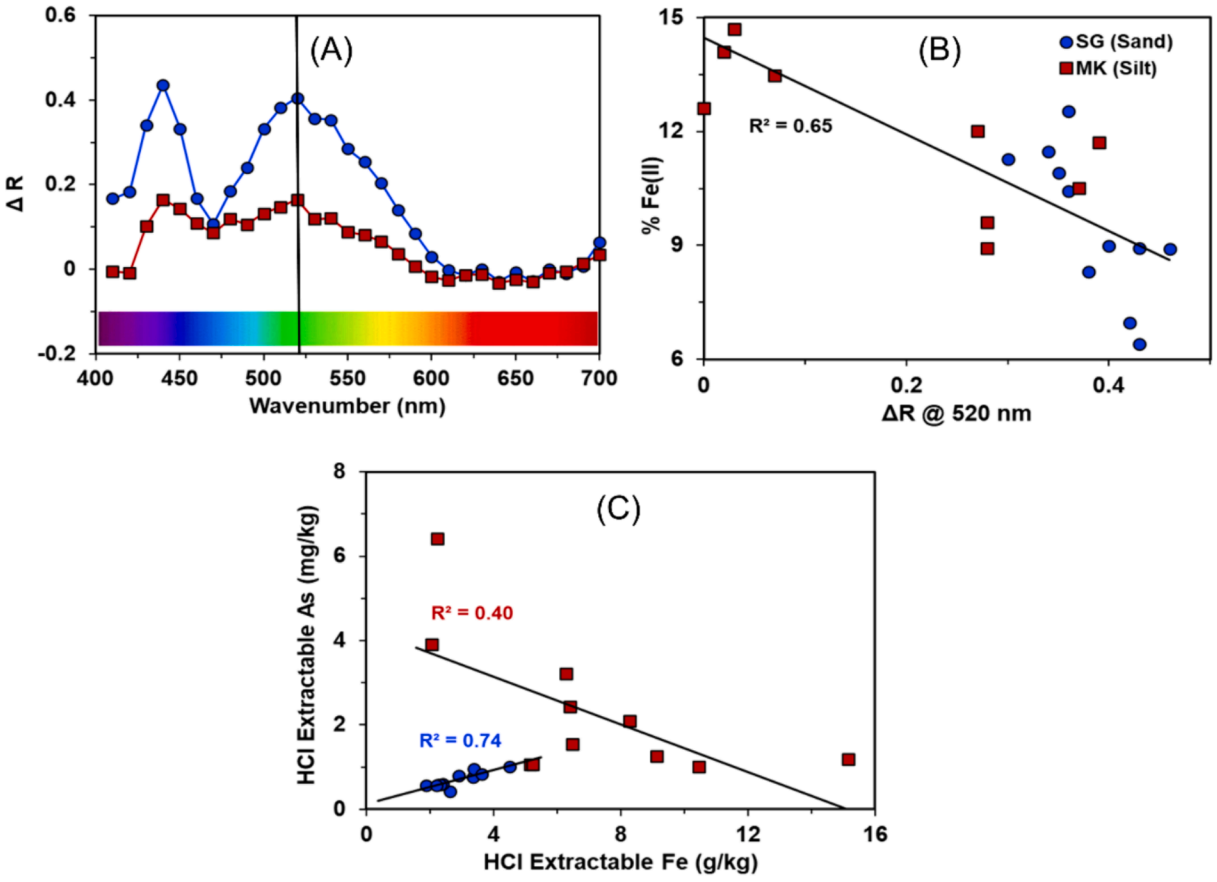

Fig. 5. (A) Spectra showing first transform derivative of the diffuse reflectance data (ΔR) along wavenumbers between 400 and 700 nm. The vertical light grey bar indicates the ΔR at 520 nm. (B) Correlation between the ΔR at 520 nm and the percentage of HCl extractable Fe(II). (C) Correlation between HCl-extractable Fe and HCl-extractable As.

Silt-Capped Site. These statistical relationships suggest that HCl-extractable As is associated with Fe(III)-oxides in the sand at the Sandy Site, whereas in the Silt-Capped Site, the As was primarily released from clay mineral hosts, such as aluminosilicate clay minerals which are commonly associated with As in the Bengal basin (Aziz et al., 2008; Charlet et al., 2007; Mihajlov et al., 2020; Varner et al., 2023).

3.4. Contrasting As mobility across two riverbanks

The contrast between the two sites in the amount and proportion of As mobilized by DI water and HCl suggests that sedimentary As was mobilized under distinct, site-specific conditions at each site (Table 1, Figs. 4 and 6). In the HZ, which can span several kilometers in width depending on regional geology, interactions between groundwater and surface water can significantly impact As mobility within shallow aquifers through fluctuating redox conditions, the advective and dispersive transport of oxidants and reductants, and the organic matter metabolization (Burrows et al., 2017; Cardenas 2015; Fischer et al., 2005; Lawson et al., 2008; Mukherjee et al., 2018; Shuai et al., 2017; Stegen et al., 2023; Varner et al., 2024, 2022; Xia et al., 2023). These interactions within HZ effectively metabolize both riverine and river-bank organic matter, thereby transforming the HZ into a biogeochemical hotspot with increased chemical reaction rates across extensive areas along river corridors (Burrows et al., 2017; Shuai et al., 2017; Stegen et al., 2023). Previous studies conducted along the Meghna River have linked As mobility to the fate of Fe(III)-oxides within the HZ of the riverbanks (Berube et al., 2018; Jung et al., 2012, 2015; Kwak et al., in press; Varner et al., 2022). At the Sandy Site along the Hooghly River in India, the strong correlation between the HCl-extractable As and Fe

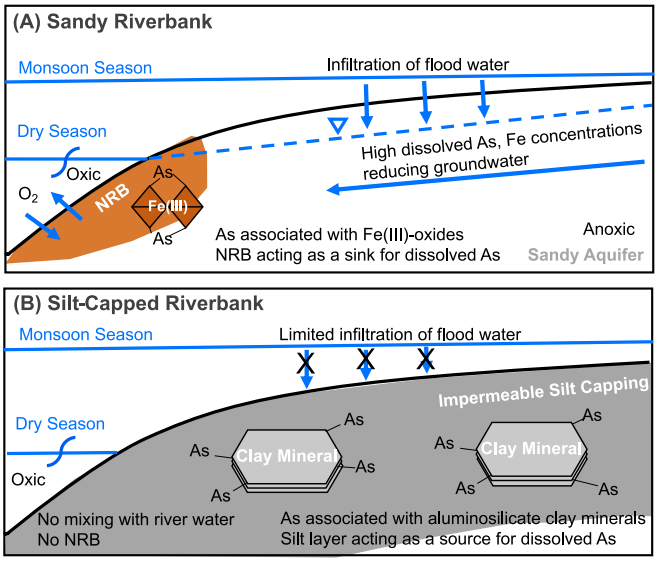

Fig. 6. Schematic model of the two study sites with contrasting lithology and the mobility of As at the two riverbanks. (A) Formation of an NRB along high-permeable sandy riverbank at the Sandy Site. The mobility of As is associated with redox condition of the riverbank and Fe(III)-oxide formation. The NRB is acting as a sink for dissolved As (B) No formation of an NRB at the Silt-Capped Site owing to limited mixing between oxidizing river water and groundwater. The mobility of As is associated with aluminosilicate clay minerals at the overlying silt layer. The silt layer can act as a source for dissolved As.

within the sand indicates the presence of As-bearing Fe-oxides within the HZ (Fig. 5). Unlike previously characterized riverbank sites along the Meghna and Red Rivers in Bangladesh and Vietnam, at the Sandy Site along the Hooghly River, the infiltrating riverine oxygen sustains oxic conditions in the sandy riverbank. This drives the active precipitation of Fe(III)-oxides which absorb As from the discharging groundwater towards the river. Evidence for As removal from porewaters was demonstrated in sandy riverbanks at several locations along the Meghna River (Berube et al., 2018; Jung et al., 2015, 2012). Berube et al. (2018) reported the presence of an NRB at a depth of approximately 1–3 m and extending 20 m from the river shoreline. At the Sandy Site, our findings demonstrate that an NRB could potentially exist within the final meter of the flow path over an approximately 6-m-wide riverbank. Furthermore, the simultaneous active sink of dissolved As and Fe in the presence of abundant DO was not previously observed along any riverbank in the Bengal Basin to the authors' knowledge.

The concentration of As-bearing Fe(III)-oxides in riverbanks deserves attention because these deposits may reductively dissolve when the riverbank becomes anoxic owing to sustained flooding or the input of labile organic matter in the sediments or as DOC in the infiltrating river water (Gao et al., 2023). Subsequently, the microbially-mediated reductive dissolution can liberate As into porewaters. The mobilized As could then potentially be transported into deeper and further aquifers during monsoon seasons (Polizzotto et al., 2005). Thus, where there is a sink for dissolved As, changing Eh or pH conditions could convert it into an important source.

At the Silt-Capped Site 80 km downstream from the Sandy site within a more tidally dominated part of the river, the lack of correlation between HCl-extractable As and Fe in the silt indicates that the As is not primarily associated with Fe(III)-oxides. There is in fact more abundant, and more mobilizable As than found in the Sandy Site where As is actively being sequestered. The elevated concentrations of water soluble and exchangeable As in the silt may be explained by its association with organic matter in the silty riverbank, which is also known to adsorb As (Wang and Mulligan, 2006). Furthermore, the high correlation between HCl-extractable Fe(II) and Al in the silt ($R^2 = 0.91$) indicates that reduced Fe predominates in more highly weathered phyllosilicates, which have higher average proportions of Al:Si than parent feldspar minerals (Stumm and Morgan, 1996). Silts and clays are known to adsorb or incorporate As in their mineral structures (Beaulieu and Savage, 2005; Charlet et al., 2007). In this case, the silt will act as a source of dissolved As across the riverbank through desorption of percolating recharge water. Lastly, if organic matter is present in concentrations high enough to drive the reduction of sulfate, sulfide precipitation may proceed to scavenge the immobilized As within the riverbank (Connolly et al., 2022; Huyen et al., 2019).

Our findings collectively suggest that the differences in As associations within riverbank sediments spanning from more riverine to more tidal dominated flow regimes of a deltaic river have contrasting impacts on the mobilization of dissolved As into the adjacent riverbank aquifer. Within sandy sediments, As is actively being sequestered onto the Fe (III)-oxide minerals under oxic conditions, whereas desorption from clay minerals and SOC in the finer grained sediments can proceed under a variety of redox states and may instead be more related to equilibrium-governed desorption (van Geen et al., 2008). When this fraction of mobilizable As from silts enters the shallow aquifer, it can cause widespread contamination (Aziz et al., 2008; Mihajlov et al., 2020).

4. Conclusion

This research aims to investigate the differences in the mineralogical association of As within riverbank sediments from two sites with contrasting surficial lithologies. At the riverbank of the Sandy Site, owing to robust tidally-driven advective mixing with oxygen-rich surface water, high levels of riverine oxygen were replenished into the HZ, maintaining oxic condition of the riverbank aquifer. Utilizing abundant introduced riverine DO as an electron acceptor, high proportions of crystalline Fe (III)-oxides (i.e., NRB) were precipitated acting as a sink for dissolved As and Fe^{2+} at the end of the groundwater flow path (Fig. 6A). This is why the concentrations of HCl-extractable sedimentary As and Fe were found to be strongly correlated in the sand. Concurrently, using the DO as primary electron acceptor, DOC was mineralized across the flow path, generating high concentrations of DIC. Calcite dissolution attenuates the acidity from the DOC mineralization, which contributed to the bulk DIC pool (Text S2). Conversely, even though the sediment from the Silt-Capped Site contained higher concentrations sedimentary As and Fe, it contained lower proportion of crystalline Fe(III)-oxide minerals than the Sandy Site sediment. The sedimentary As in the silt was correlated with aluminosilicate clay minerals rather than Fe(III)-oxides (Fig. 6B). These minerals in the silt can potentially act as source of dissolved As through equilibrium-regulated desorption of percolating recharge water across broad floodplains. The surficial lithology of a riverbank under influence of tidal fluctuations plays an important role in regulating the mobility of As and its chemical association to mineral groups within shallow riverbank sediments. This study provided better understanding of the varying sinks and sources of dissolved As at surface water-groundwater interfaces in riverbanks along the riverine to tidal continuum.

CRediT authorship contribution statement

Kyungwon Kwak: Writing – review & editing, Writing – original draft, Visualization, Validation, Resources, Project administration, Methodology, Investigation, Funding acquisition, Formal analysis, Data curation, Conceptualization. **Thomas S. Varner:** Writing – review & editing, Writing – original draft, Visualization, Validation, Resources, Project administration, Methodology, Investigation, Funding acquisition, Formal analysis, Data curation, Conceptualization. **Saptarshi Saha:** Resources, Methodology, Investigation, Data curation. **Mesbah U. Bhuiyan:** Resources, Methodology, Investigation, Data curation. **Harshad V. Kulkarni:** Writing – review & editing, Validation, Supervision, Resources, Methodology, Investigation, Formal analysis, Data curation, Conceptualization. **Ananya Mukhopadhyay:** Writing – review & editing, Validation, Supervision, Resources, Project administration, Methodology, Investigation, Data curation. **Saugata Datta:** Writing – review & editing, Validation, Supervision, Resources, Project administration, Methodology, Investigation, Funding acquisition, Conceptualization. **Peter S. K. Knappett:** Writing – review & editing, Validation, Supervision, Resources, Project administration, Methodology, Funding acquisition, Formal analysis, Conceptualization.

Declaration of competing interest

The authors declare that they have no known competing financial interests or personal relationships that could have appeared to influence the work reported in this paper.

Data availability

The datasets analyzed during this study are openly available in HydroShare at https://doi.org/10.4211/hs.e47c60a00425431aafeffe9046eaf902. All other datasets will be made available on request.

Acknowledgements

This project is funded by a Pathfinder Graduate Student Fellowship to K. Kwak, sponsored by the CUAHSI with support from the National Science Foundation (NSF) Cooperative Agreement No. EAR-1849458 and a Fulbright Student Fellowship to T. Varner, sponsored by the United States-India Education Foundation (USIEF). K. Kwak and T. Varner and their field and analytical costs were further supported by the NSF on grants EAR-1852652 and 1852651 to P. Knappett and S. Datta, respectively. We would like to thank Deeksha Kumari from IIT Mandi for

the assistance with the laboratory analyses. We appreciate the editor and two anonymous reviewers for their valuable comments that greatly improved the manuscript.

Appendix A. Supplementary data

Supplementary data to this article can be found online at https://doi.org/10.1016/j.jhydrol.2024.131773.

References

Aftabtalab, A., Rinklebe, J., Shaheen, S.M., Niazi, N.K., Moreno-Jiménez, E., Schaller, J., Knorr, K.H., 2022. Review on the interactions of arsenic, iron (oxy)(hydr)oxides, and dissolved organic matter in soils, sediments, and groundwater in a ternary system. Chemosphere 286. https://doi.org/10.1016/j.chemosphere.2021.131790.

Appelo, C.A.J., Postma, D., 2005. Geochemistry, groundwater and pollution, 2nd ed. CRC Press.

Aziz, Z., Van Geen, A., Stute, M., Versteeg, R., Horneman, A., Zheng, Y., Goodbred, S., Steckler, M., Weinman, B., Gavrieli, I., Hoque, M.A., Shamsudduha, M., Ahmed, K. M., 2008. Impact of local recharge on arsenic concentrations in shallow aquifers inferred from the electromagnetic conductivity of soils in Araihazar, Bangladesh. Water Resour. Res. 44, 1–15. https://doi.org/10.1029/2007WR006000.

Beaulieu, B.T., Savage, K.S., 2005. Arsenate adsorption structures on aluminum oxide and phyllosilicate mineral surfaces in smelter-impacted soils. Environ. Sci. Technol. 39, 3571–3579. https://doi.org/10.1021/es048836f.

Berube, M., Jewell, K., Myers, K.D., Knappett, P.S.K., Shuai, P., Hossain, A., Lipsi, M., Hossain, S., Hossain, A., Aitkenhead-Peterson, J., Ahmed, K.M., Datta, S., 2018. The fate of arsenic in groundwater discharged to the Meghna River, Bangladesh. Environ. Chem. 15, 29–45. https://doi.org/10.1071/EN17104.

Bhowmick, S., Nath, B., Halder, D., Biswas, A., Majumder, S., Mondal, P., Chakraborty, S., Nriagu, J., Bhattacharya, P., Iglesias, M., Roman-Ross, G., Guha Mazumder, D., Bundschuh, J., Chatterjee, D., 2013. Arsenic mobilization in the aquifers of three physiographic settings of West Bengal, India: Understanding geogenic and anthropogenic influences. J. Hazard. Mater. 262, 915–923. https://doi.org/10.1016/j.jhazmat.2012.07.014.

Bufe, A., Hovius, N., Emberson, R., Rugenstein, J.K.C., Galy, A., Hassenruck-Gudipati, H. J., Chang, J.M., 2021. Co-variation of silicate, carbonate and sulfide weathering drives CO2 release with erosion. Nat. Geosci. 14, 211–216. https://doi.org/10.1038/s41561-021-00714-3.

Burrows, R.M., Rutlidge, H., Bond, N.R., Eberhard, S.M., Auhl, A., Andersen, M.S., et al., 2017. High rates of organic carbon processing in the hyporheic zone of intermittent streams. Sci. Rep. 7 (1), 1–12. https://doi.org/10.1038/s41598-017-12957-5.

Cardenas, M.B., 2015. Hyporheic zone hydrologic science: A historical account of its emergence and a prospectus. Water Resour. Res. 51, 3601–3616. https://doi.org/10.1002/2015WR017028.

Chakraborti, D., Das, B., Rahman, M.M., Chowdhury, U.K., Biswas, B., Goswami, A.B., Nayak, B., Pal, A., Sengupta, M.K., Ahamed, S., Hossain, A., Basu, G., Roychowdhury, T., Das, D., 2009. Status of groundwater arsenic contamination in the state of West Bengal, India: A 20-year study report. Mol. Nutr. Food Res. 53, 542–551. https://doi.org/10.1002/mnfr.200700517.

Chakraborty, M., Mukherjee, A., Ahmed, K.M., 2015. A Review of Groundwater Arsenic in the Bengal Basin, Bangladesh and India: from Source to Sink. Curr. Pollut. Reports 1, 220–247. https://doi.org/10.1007/s40726-015-0022-0.

Chakraborty, M., Sarkar, S., Mukherjee, A., Shamsudduha, M., Ahmed, K.M., Bhattacharya, A., Mitra, A., 2020. Modeling regional-scale groundwater arsenic hazard in the transboundary Ganges River Delta, India and Bangladesh: Infusing physically-based model with machine learning. Sci. Total Environ. 748, 141107 https://doi.org/10.1016/j.scitotenv.2020.141107.

Charlet, L., Chakraborty, S., Appelo, C.A.J., Roman-Ross, G., Nath, B., Ansari, A.A., Lanson, M., Chatterjee, D., Mallik, S.B., 2007. Chemodynamics of an arsenic "hotspot" in a West Bengal aquifer: A field and reactive transport modeling study. Appl. Geochemistry 22, 1273–1292. https://doi.org/10.1016/j.apgeochem.2006.12.022.

Chowdhury, U.K., Biswas, B.K., Chowdhury, T.R., Samanta, G., Mandal, B.K., Basu, G.C., Chanda, C.R., Lodh, D., Saha, K.C., Mukherjee, S.K., Roy, S., Kabir, S., Quamruzzaman, Q., Chakraborti, D., 2000. Groundwater arsenic contamination in Bangladesh and West Bengal, India. Environ. Health Perspect. 108, 393–397. https://doi.org/10.1289/ehp.00108393.

Chugh, R.S., 1961. Tides in Hooghly river. Int. Assoc. Sci. Hydrol. Bull. 6, 10–26. https://doi.org/10.1080/02626666109493212.

Connolly, C.T., Stahl, M.O., DeYoung, B.A., Bostick, B.C., 2022. Surface flooding as a key driver of groundwater arsenic contamination in Southeast Asia. Environ. Sci. Technol. 56, 928–937. https://doi.org/10.1021/acs.est.1c05955.

Datta, S., Mailloux, B., Jung, H.B., Hoque, M.A., Stute, M., Ahmed, K.M., Zheng, Y., 2009. Redox trapping of arsenic during groundwater discharge in sediments from the Meghna riverbank in Bangladesh. Proc. Natl. Acad. Sci. U. S. A. 106, 16930–16935. https://doi.org/10.1073/pnas.0908168106.

Deb, S., Chakraborty, A., 2013. Observational analysis of the Hooghly Estuarine features and tidal effects using a high resolution biophysical model. Int. Geosci. Remote Sens. Symp. 1587–1590 https://doi.org/10.1109/IGARSS.2013.6723093.

Deb, S., Chakraborty, A., 2015. Simulating the effects of tidal dynamics on the biogeochemistry of the Hooghly estuary. IEEE J. Sel. Top. Appl. Earth Obs. Remote Sens. 8, 130–140. https://doi.org/10.1109/JSTARS.2014.2348313.

Desbarats, A.J., Koenig, C.E.M., Pal, T., Mukherjee, P.K., Beckie, R.D., 2014. Groundwater flow dynamics and arsenic source characterization in an aquifer system of West Bengal, India. Water Resour. Res. 50, 4974–5002. https://doi.org/10.1002/2013WR014034.

Dixit, S., Hering, J.G., 2003. Comparison of arsenic(V) and arsenic(III) sorption onto iron oxide minerals: Implications for arsenic mobility. Environ. Sci. Technol. 37, 4182–4189. https://doi.org/10.1021/es030309t.

DPHE/BGS, 2001. Arsenic contamination of groundwater in Bangladesh, British Geological Survey Technical Report WC/00/19.

Erban, L.E., Gorelick, S.M., Zebker, H.A., Fendorf, S., 2013. Release of arsenic to deep groundwater in the Mekong Delta, Vietnam, linked to pumping-induced land subsidence. Proc. Natl. Acad. Sci. U. S. A. 110, 13751–13756. https://doi.org/10.1073/pnas.1300503110.

Fellman, J.B., D'Arnore, D.V., Hood, E., 2008. An evaluation of freezing as a preservation technique for analyzing dissolved organic C, N, and P in surface water samples. Sci. Total Environ. 392, 305–312. https://doi.org/10.1016/j.scitotenv.2007.11.027.

Fendorf, S., Michael, H.A., Van Geen, A., 2010. Spatial and temporal variations of groundwater arsenic in South and Southeast Asia. Science (80-.) 328, 1123–1127. https://doi.org/10.1126/science.1172974.

Fischer, H., Kloep, F., Wilzcek, S., Pusch, M.T., 2005. A river's liver - Microbial processes within the hyporheic zone of a large lowland river. Biogeochemistry 76 (2), 349–371. https://doi.org/10.1007/s10533-005-6896-y.

Gao, Z., Guo, H., Chen, D., Yu, C., He, C., Shi, Q., Qiao, W., Kersten, M., 2023. Transformation of dissolved organic matter and related arsenic mobility at a surface water-groundwater interface in the Hetao Basin, China. Environ. Pollut. 334, 122202 https://doi.org/10.1016/j.envpol.2023.122202.

Gao, C., Sander, M., Agethen, S., Knorr, K.H., 2019. Electron accepting capacity of dissolved and particulate organic matter control CO2 and CH4 formation in peat soils. Geochim. Cosmochim. Acta 245, 266–277. https://doi.org/10.1016/j.gca.2018.11.004.

Goodbred, S.L., Kuehl, S.A., Steckler, M.S., Sarker, M.H., 2003. Controls on facies distribution and stratigraphic preservation in the Ganges-Brahmaputra delta sequence. Sediment. Geol. 155, 301–316. https://doi.org/10.1016/S0037-0738(02)00184-7.

Gran, G., 1952. Determination of the equivalence point in potentiometric acid-base titrations. Analyst 77, 661–671.

Harvey, C.F., Swartz, C.H., Badruzzaman, A.B.M., Keon-Blute, N., Yu, W., Ali, M.A., Jay, J., Beckie, R., Niedan, V., Brabander, D., Oates, P.M., Ashfaque, K.N., Islam, S., Hemond, H.F., Ahmed, M.F., 2002. Arsenic mobility and groundwater extraction in Bangladesh. Science (80-.) 298, 1602–1606. https://doi.org/10.1126/science.1076978.

Horneman, A., van Geen, A., Kent, D.V., Mathe, P.E., Zheng, Y., Dhar, R.K., O'Connell, S., Hoque, M.A., Aziz, Z., Shamsudduha, M., Seddique, A.A., Ahmed, K.M., 2004. Decoupling of As and Fe release to Bangladesh groundwater under reducing conditions. Part I: Evidence from sediment profiles. Geochim. Cosmochim. Acta 68, 3459–3473. https://doi.org/10.1016/j.gca.2004.01.026.

Huang, Y., Knappett, P.S.K., Berube, M., Datta, S., Cardenas, M.B., Rhodes, K.A., Dimova, N.T., Choudhury, I., Ahmed, K.M., van Geen, A., 2022. Mass fluxes of dissolved arsenic discharging to the Meghna River are sufficient to account for the mass of arsenic in riverbank sediments. J. Contam. Hydrol. 251, 104068 https://doi.org/10.1016/j.jconhyd.2022.104068.

Human Rights Watch, 2016. Nepotism and neglect: The Failing Response to Arsenic in the Drinking Water of Bangladesh's Rural Poor.

Huyen, D.T., Tabelin, C.B., Thuan, H.M., Dang, D.H., Truong, P.T., Vongphuthone, B., Kobayashi, M., Igarashi, T., 2019. The solid-phase partitioning of arsenic in unconsolidated sediments of the Mekong Delta, Vietnam and its modes of release under various conditions. Chemosphere 233, 512–523. https://doi.org/10.1016/j.chemosphere.2019.05.235.

Islam, A., Guchhait, S.K., 2020. Characterizing cross-sectional morphology and channel inefficiency of lower Bhagirathi River, India, in post-Farakka barrage condition, Natural Hazards. Springer Netherlands. 10.1007/s11069-020-04156-9.

Islam, F.S., Gault, A.G., Boothman, C., Polya, D.A., Chamok, J.M., Chatterjee, D., Lloyd, J.R., 2004. Role of metal-reducing bacteria in arsenic release from Bengal delta sediments. Nature 430, 68–71. https://doi.org/10.1038/nature02638.

Islam, A., Guchhait, S.K., 2017. Analysing the influence of Farakka Barrage Project on channel dynamics and meander geometry of Bhagirathi river of West Bengal, India. Arab. J. Geosci. 10 https://doi.org/10.1007/s12517-017-3004-2.

Jewell, K., Myers, K.D., Lipsi, M., Hossain, S., Datta, S., Cardenas, M.B., Aitkenhead-peterson, J., Varner, T., Kwak, K., Raymond, A., Akhter, S.H., Ahmed, K.M., Knappett, P.S.K., 2023. Redox trapping of arsenic in hyporheic zones modified by silicate weathering beneath floodplains. Geochem. Appl. https://doi.org/10.1016/j.apgeochem.2023.105831.

Johnston, S.G., Diwakar, J., Burton, E.D., 2015. Arsenic solid-phase speciation in an alluvial aquifer system adjacent to the Himalayan Forehills, Nepal. Chem. Geol. 419, 55–66. https://doi.org/10.1016/j.chemgeo.2015.10.035.

Jung, H.B., Bostick, B.C., Zheng, Y., 2012. Field, experimental, and modeling study of arsenic partitioning across a redox transition in a Bangladesh aquifer. Environ. Sci. Technol. 46, 1388–1395. https://doi.org/10.1021/es2032967.

Jung, H.B., Zheng, Y., Rahman, M.W., Rahman, M.M., Ahmed, K.M., 2015. Redox zonation and oscillation in the hyporheic zone of the Ganges-Brahmaputra-Meghna Delta: Implications for the fate of groundwater arsenic during discharge. Appl. Geochem. 63, 647–660. https://doi.org/10.1016/j.apgeochem.2015.09.001.

Kanuri, V.V., Saha, R., Raghuvanshi, S.P., Singh, A.K., Chakraborty, B.D., Kumar, V.K., Mohapatra, S.C., Vidyarthi, A.K., Sudhakar, A., Saxena, R.C., 2019. Sewage fluxes and seasonal dynamics of physicochemical characteristics of the Bhagirathi-Hooghly

River from the lower stretch of River Ganges, India. Chem. Ecol. 36, 30–47. https://doi.org/10.1080/02757540.2019.1692826.
Kaufman, M.H., Cardenas, M.B., Buttles, J., Kessler, A.J., Cook, P.L.M., 2017. Hyporheic hot moments: Dissolved oxygen dynamics in the hyporheic zone in response to surface flow perturbations. Water Resour. Res. 53, 6642–6662. https://doi.org/10.1002/2016WR020296.
Kazmierczak, J., Postma, D., Dang, T., Hoang, H.V., Larsen, F., Hass, A.E., Hoffmann, A. H., Fensholt, R., Pham, N.Q., Jakobsen, R., 2022. Groundwater arsenic content related to the sedimentology and stratigraphy of the Red River delta, Vietnam. Sci. Total Environ. 814, 152641 https://doi.org/10.1016/j.scitotenv.2021.152641.
Khan, A., Chatterjee, S., Bisai, D., 2015. On the long-term variability of temperature trends and changes in surface air temperature in Kolkata Weather Observatory, West Bengal, India. Meteorol. Hydrol. Water Manag. 3, 9–16. https://doi.org/10.26491/mhwm/59336.
Kuehl, S.A., Allison, M.A., Goodbred, S.L., Kudrass, H., 2005. The Ganges-Brahmaputra Delta. River Deltas–Concepts, Model. Examples. 10.2110/pec.05.83.0413.
Kwak, K., Varner, T.S., Nguyen, W., Kulkarni, H.V., Buskirk, R., Huang, Y., Saeed, A., Hosain, A., Aitkenhead-Peterson, J., Ahmed, K.M., Akhter, S.H., Cardenas, M.B., Datta, S., Knappett, P.S.K., In Press. Hotspots of Dissolved Arsenic Generated from Buried Silt Layers along Fluctuating Rivers. Environ. Sci. Technol.
Larsen, F., Pham, N.Q., Dang, N.D., Postma, D., Jessen, S., Pham, V.H., Nguyen, T.B., Trieu, H.D., Tran, L.T., Nguyen, H., Chambon, J., Nguyen, H.V., Ha, D.H., Hue, N.T., Duc, M.T., Refsgaard, J.C., 2008. Controlling geological and hydrogeological processes in an arsenic contaminated aquifer on the Red River flood plain, Vietnam. Appl. Geochem. 23, 3099–3115. https://doi.org/10.1016/j.apgeochem.2008.06.014.
Lau, M.P., Sander, M., Gelbrecht, J., Hupfer, M., 2015. Solid phases as important electron acceptors in freshwater organic sediments. Biogeochemistry 123, 49–61. https://doi.org/10.1007/s10533-014-0052-5.
Lawson, M., Ballentine, C.J., Polya, D.A., Boyce, A.J., Mondal, D., Chatterjee, D., et al., 2008. The geochemical and isotopic composition of ground waters in West Bengal: tracing ground-surface water interaction and its role in arsenic release. Mineral. Mag. 72 (1), 441–444. https://doi.org/10.1180/minmag.2008.072.1.441.
Mackay, A.A., Gan, P., Yu, R., Smets, B.F., 2014. Seasonal arsenic accumulation in stream sediments at a groundwater discharge zone. Environ. Sci. Technol. 48, 920–929. https://doi.org/10.1021/es402552u.
Mailloux, B.J., Trembath-Reichert, E., Cheung, J., Watson, M., Stute, M., Freyer, G.A., Ferguson, A.S., Ahmed, K.M., Alam, M.J., Buchholz, B.A., Thomas, J., Layton, A.C., Zheng, Y., Bostick, B.C., Van Geen, A., 2013. Advection of surface-derived organic carbon fuels microbial reduction in Bangladesh groundwater. Proc. Natl. Acad. Sci. U. S. A. 110, 5331–5335. https://doi.org/10.1073/pnas.1213141110.
McArthur, J.M., Ravenscroft, P., Safiulla, S., Thirlwall, M.F., 2001. Arsenic in groundwater: Testing pollution mechanisms for sedimentary aquifers in Bangladesh. Water Resour. Res. 37, 109–117. https://doi.org/10.1029/2000WR900270.
McArthur, J.M., Banerjee, D.M., Hudson-Edwards, K.A., Mishra, R., Purohit, R., Ravenscroft, P., Cronin, A., Howarth, R.J., Chatterjee, A., Talukder, T., Lowry, D., Houghton, S., Chadha, D.K., 2004. Natural organic matter in sedimentary basins and its relation to arsenic in anoxic ground water: The example of West Bengal and its worldwide implications. Appl. Geochem. 19, 1255–1293. https://doi.org/10.1016/j.apgeochem.2004.02.001.
McArthur, J.M., Banerjee, D.M., Sengupta, S., Ravenscroft, P., Klump, S., Sarkar, A., Disch, B., Kipfer, R., 2010. Migration of As, and 3H/3He ages, in groundwater from West Bengal: Implications for monitoring. Water Res. 44, 4171–4185. https://doi.org/10.1016/j.watres.2010.05.010.
McArthur, J.M., Sikdar, P.K., Leng, M.J., Ghosal, U., Sen, I., 2018. Groundwater Quality beneath an Asian Megacity on a Delta: Kolkata's (Calcutta's) Disappearing Arsenic and Present Manganese. Environ. Sci. Technol. 52, 5161–5172. https://doi.org/10.1021/acs.est.7b04996.
Mihajlov, I., Mozumder, M.R.H., Bostick, B.C., Stute, M., Mailloux, B.J., Knappett, P.S.K., Choudhury, I., Ahmed, K.M., Schlosser, P., van Geen, A., 2020. Arsenic contamination of Bangladesh aquifers exacerbated by clay layers. Nat. Commun. 11 https://doi.org/10.1038/s41467-020-16104-z.
Mirza, M.M.Q., 1997. Modifications hydrologiques du système du Gange au Bangladesh depuis la construction du barrage de Farakka. Hydrol. Sci. J. 42, 613–631. https://doi.org/10.1080/02626669709492062.
Mondal, P., Schintu, M., Marras, B., Bettoschi, A., Marrucci, A., Sarkar, S. K., et al., 2020. Geochemical fractionation and risk assessment of trace elements in sediments from tide- dominated Hooghly (Ganges) River Estuary, India. Chem. Geol., 532(August 2019), 119373. 10.1016/j.chemgeo.2019.119373.
Mondal, P., Reichelt-Brushett, A.J., Jonathan, M.P., Sujitha, S.B., Sarkar, S.K., 2018. Pollution evaluation of total and acid-leachable trace elements in surface sediments of Hooghly River Estuary and Sundarban Mangrove Wetland (India). Environ. Sci. Pollut. Res. 25 (6), 5681–5699. https://doi.org/10.1007/s11356-017- 0915-0.
Mozumder, M.R.H., Michael, H.A., Mihajlov, I., Khan, M.R., Knappett, P.S.K., Bostick, B. C., Mailloux, B.J., Ahmed, K.M., Choudhury, I., Koffman, T., Ellis, T., Whaley-Martin, K., San Pedro, R., Slater, G., Stute, M., Schlosser, P., van Geen, A., 2020. Origin of groundwater arsenic in a rural pleistocene aquifer in bangladesh depressurized by distal municipal pumping. Water Resour. Res. 56, 1–26. https://doi.org/10.1029/2020WR027178.
Mukherjee, A., Fryar, A.E., Rowe, H.D., 2007. Regional-scale stable isotopic signatures of recharge and deep groundwater in the arsenic affected areas of West Bengal. India. J. Hydrol. 334, 151–161. https://doi.org/10.1016/j.jhydrol.2006.10.004.
Mukherjee, A., Bhanja, S.N., Wada, Y., 2018a. Groundwater depletion causing reduction of baseflow triggering Ganges river summer drying. Scientific Reports 8 (1), 1–9. https://doi.org/10.1038/s41598-018-30246-7.
Mukherjee, A., Fryar, A.E., Eastridge, E.M., Nally, R.S., Chakraborty, M., Scanlon, B.R., 2018b. Controls on high and low groundwater arsenic on the opposite banks of the lower reaches of River Ganges, Bengal basin. India. Sci. Total Environ. 645, 1371–1387. https://doi.org/10.1016/j.scitotenv.2018.06.376.
Mukhopadhyay, A., Acharyya, R., Habel, M., Pal, I., Pramanick, N., Hati, J.P., Sanyal, M. K., Ghosh, T., 2023. Upstream river erosion vis-a-vis sediments variability in Hugli Estuary, India: A geospatial approach. Water (Switzerland) 15, 1–26. https://doi.org/10.3390/w15071285.
Murshed, S.B., Rahman, M.R., Kaluarachchi, J.J., 2019. Changes in hydrology of the Ganges delta of Bangladesh and corresponding impacts on water resources. J. Am. Water Resour. Assoc. 55, 800–823. https://doi.org/10.1111/1752-1688.12775.
Musial, C.T., Sawyer, A.H., Barnes, R.T., Bray, S., Knights, D., 2016. Surface water-groundwater exchange dynamics in a tidal freshwater zone. Hydrol. Process. 30, 739–750. https://doi.org/10.1002/hyp.10623.
Nagorski, S.A., Moore, J.N., 1999. Arsenic mobilization in the hyporheic zone of a contaminated stream. Water Resour. Res. 35, 3441–3450. https://doi.org/10.1029/1999WR900204.
Nickson, R.T., Mcarthur, J.M., Ravenscroft, P., Burgess, W.G., Ahmed, K.M., 2000. Mechanism of arsenic release to groundwater, Bangladesh and West Bengal. Appl. Geochem. 15, 403–413. https://doi.org/10.1016/S0883-2927(99)00086-4.
Parsons, C.T., Couture, R.M., Omoregie, E.O., Bardelli, F., Greneche, J.M., Roman-Ross, G., Charlet, L., 2013. The impact of oscillating redox conditions: Arsenic immobilisation in contaminated calcareous floodplain soils. Environ. Pollut. 178, 254–263. https://doi.org/10.1016/j.envpol.2013.02.028.
Paszkowski, A., Goodbred Jr., S., Borgomeo, E., Khan, M.S.A., Hall, J.W., 2021. Geomorphic change in the Ganges – Brahmaputra – Meghna delta. Nat. Rev Earth Environ. 1.
Planer-Friedrich, B., Härtig, C., Lissner, H., Steinborn, J., Süß, E., Qumrul Hassan, M., Zahid, A., Alam, M., Merkel, B., 2012. Organic carbon mobilization in a Bangladesh aquifer explained by seasonal monsoon-driven storativity changes. Appl. Geochem. 27, 2324–2334. https://doi.org/10.1016/j.apgeochem.2012.08.005.
Polizzotto, M.L., Harvey, C.F., Sutton, S.R., Fendorf, S., 2005. Processes conducive to the release and transport of arsenic into aquifers of Bangladesh. Proc. Natl. Acad. Sci. U. S. A. 102, 18819–18823. https://doi.org/10.1073/pnas.0509539103.
Polizzotto, M.L., Kocar, B.D., Benner, S.G., Sampson, M., Fendorf, S., 2008. Near-surface wetland sediments as a source of arsenic release to ground water in Asia. Nature 454, 505–508. https://doi.org/10.1038/nature07093.
Postma, D., Larsen, F., Minh Hue, N.T., Duc, M.T., Viet, P.H., Nhan, P.Q., Jessen, S., 2007. Arsenic in groundwater of the Red River floodplain, Vietnam: Controlling geochemical processes and reactive transport modeling. Geochim. Cosmochim. Acta 71, 5054–5071. https://doi.org/10.1016/j.gca.2007.08.020.
Postma, D., Jessen, S., Hue, N.T.M., Duc, M.T., Koch, C.B., Viet, P.H., Nhan, P.Q., Larsen, F., 2010. Mobilization of arsenic and iron from Red River floodplain sediments, Vietnam. Geochim. Cosmochim. Acta 74, 3367–3381. https://doi.org/10.1016/j.gca.2010.03.024.
Potter, B.B., Wimsatt, J.C., 2005. Method 415.3 -measurement of total organic carbon, dissolved organic carbon and specific uv absorbance at 254 nm in source water and drinking water. Washington, DC.
Sankar, M.S., Vega, M.A., Defoe, P.P., Kibria, M.G., Ford, S., Telfeyan, K., Neal, A., Mohajerin, T.J., Hettiarachchi, G.M., Barua, S., Hobson, C., Johannesson, K., Datta, S., 2014. Elevated arsenic and manganese in groundwaters of Murshidabad, West Bengal, India. Sci. Total Environ. 488–489, 570–579. https://doi.org/10.1016/j.scitotenv.2014.02.077.
Sarkar, S.K., Mondal, P., Biswas, J.K., Kwon, E.E., Ok, Y.S., Rinklebe, J., 2017. Trace elements in surface sediments of the Hooghly (Ganges) estuary: distribution and contamination risk assessment. Environ. Geochem. Health 39 (6), 1245–1258. https://doi.org/10.1007/s10653-017-9952-3.
Schittich, A.R., Wünsch, U.J., Kulkarni, H.V., Battistel, M., Bregnhøj, H., Stedmon, C.A., McKnight, U.S., 2018. Investigating fluorescent organic-matter composition as a key predictor for arsenic mobility in groundwater aquifers. Environ. Sci. Technol. 52, 13027–13036. https://doi.org/10.1021/acs.est.8b04070.
Senn, A.C., Hug, S.J., Kaegi, R., Hering, J.G., Voegelin, A., 2018. Arsenate co-precipitation with Fe(II) oxidation products and retention or release during precipitate aging. Water Res. 131, 334–345. https://doi.org/10.1016/j.watres.2017.12.038.
Shuai, P., Cardenas, M.B., Neilson, B.T., Knappett, P.S.K., Bennett, P.C., Neilson, B.T., 2017. Denitrification in the banks of fluctuating rivers: The effects of river stage amplitude, sediment hydraulic conductivity and dispersivity, and ambient groundwater flow. Water Resour. Res. 53, 7951–7967. https://doi.org/10.1002/2017WR020610.
Smedley, P.L., Kinniburgh, D.G., 2002. A review of the source, behaviour and distribution of arsenic in natural waters. Appl. Geochem. 17, 517–568. https://doi.org/10.1016/S0883-2927(02)00018-5.
Smith, R., Knight, R., Fendorf, S., 2018. Overpumping leads to California groundwater arsenic threat. Nat. Commun. 9, 1–6. https://doi.org/10.1038/s41467-018-04475-3.
Smith, A.H., Lingas, E.O., Rahman, M., 2000. Contamination of Drinking Water by Arsenic in Bangladesh: A Public Health Emergency. Bulletin of the World Health Organization 78: Contamination of drinking-water by arsenic in Bangladesh: a public health emergency. World Heal. Organ. Bull. World Heal. Organ. 78, 1093–1103.
Stahl, M.O., Harvey, C.F., van Geen, A., Sun, J., 2016. River bank geomorphology controls groundwater arsenic concentrations in aquifers adjacent to the Red River, Hanoi Vietnam. Water Resour. Res. 52, 6321–6334. https://doi.org/10.1002/2016WR018891.
Stegen, J.C., Garayburu-Caruso, V.A., Danczak, R.E., Goldman, A.E., Renteria, L., Torgeson, J.M., Hager, J., 2023. Maximum respiration rates in hyporheic zone sediments are primarily constrained by organic carbon concentration and

secondarily by organic matter chemistry. Biogeosciences 20 (14), 2857–2867. https://doi.org/10.5194/bg-20-2857-2023.

Stopelli, E., Duyen, V.T., Prommer, H., Glodowska, M., Kappler, A., Schneider, M., Eiche, E., Lightfoot, A.K., Schubert, C.J., Trang, P.K.T., Viet, P.H., Kipfer, R., Winkel, L.H.E., Berg, M., 2021. Carbon and methane cycling in arsenic-contaminated aquifers. Water Res. 200 https://doi.org/10.1016/j.watres.2021.117300.

Stumm, W., Morgan, J.J., 1996. Aquatic Chemistry: Chemical Equilibria and Rates in Natural Waters. Wiley-Interscience, New York.

Stute, M., Zheng, Y., Schlosser, P., Horneman, A., Dhar, R.K., Datta, S., Hoque, M.A., Seddique, A.A., Shamsudduha, M., Ahmed, K.M., Van Geen, A., 2007. Hydrological control of As concentrations in Bangladesh groundwater. Water Resour. Res. 43, 1–11. https://doi.org/10.1029/2005WR004499.

Trifuoggi, M., Ferrara, L., Toscanesi, M., Mondal, P., Ponniah, J.M., Sarkar, S.K., Arienzo, M., 2022. Spatial distribution of trace elements in surface sediments of Hooghly (Ganges) river estuary in West Bengal, India. *Environ. Sci. Pollut. Res.* 29 (5), 6929–6942. https://doi.org/10.1007/s11356-021-15918-8.

van Geen, A., Rose, J., Thoral, S., Garnier, J.M., Zheng, Y., Bottero, J.Y., 2004. Decoupling of As and Fe release to Bangladesh groundwater under reducing conditions. Part II: Evidence from sediment incubations. Geochim. Cosmochim. Acta 68, 3475–3486. https://doi.org/10.1016/j.gca.2004.02.014.

van Geen, A., Zheng, Y., Goodbred, S., Horneman, A., Aziz, Z., Cheng, Z., Stute, M., Mailloux, B., Weinman, B., Hoque, M.A., Seddique, A.A., Hossain, M.S., Chowdhury, S.H., Ahmed, K.M., 2008. Flushing history as a hydrogeological control on the regional distribution of arsenic in shallow groundwater of the Bengal basin. Environ. Sci. Technol. 42, 2283–2288. https://doi.org/10.1021/es702316k.

Varner, T.S., Kulkarni, H.V., Nguyen, W., Kwak, K., Cardenas, M.B., Knappett, P.S.K., Ojeda, A.S., Malina, N., Bhuiyan, M.U., Ahmed, K.M., Datta, S., 2022. Contribution of sedimentary organic matter to arsenic mobilization along a potential natural reactive barrier (NRB) near a river: The Meghna river, Bangladesh. Chemosphere 308, 136289. https://doi.org/10.1016/j.chemosphere.2022.136289.

Varner, T.S., Kulkarni, H.V., Bhuiyan, M.U., Cardenas, M.B., Knappett, P.S.K., Datta, S., 2023. Mineralogical associations of sedimentary arsenic within a contaminated aquifer determined through thermal treatment and spectroscopy. Minerals 13. https://doi.org/10.3390/min13070889.

Varner, T.S., Kulkarni, H.V., Kwak, K., Cardenas, M.B., Knappett, P.S.K., Datta, S., 2024. Diverse sedimentary organic matter within the river-aquifer interface drives arsenic mobility along the Meghna River Corridor in Bangladesh. Appl. Geochem. 161 (January), 105883 https://doi.org/10.1016/j.apgeochem.2023.105883.

Wallis, I., Prommer, H., Berg, M., Siade, A.J., Sun, J., Kipfer, R., 2020. The river–groundwater interface as a hotspot for arsenic release. Nat. Geosci. 13, 288–295. https://doi.org/10.1038/s41561-020-0557-6.

Wang, S., Mulligan, C.N., 2006. Natural attenuation processes for remediation of arsenic contaminated soils and groundwater. J. Hazard. Mater. 138, 459–470. https://doi.org/10.1016/j.jhazmat.2006.09.048.

Weinman, B., Goodbred, S.L., Zheng, Y., Aziz, Z., Steckler, M., van Geen, A., Singhvi, A. K., Nagar, Y.C., 2008. Contributions of floodplain stratigraphy and evolution to the spatial patterns of groundwater arsenic in Araihazar, Bangladesh. Bull. Geol. Soc. Am. 120, 1567–1580. https://doi.org/10.1130/B26209.1.

Wilson, C.A., Goodbred, S.L., 2015. Construction and maintenance of the Ganges-Brahmaputra-Meghna delta: Linking process, morphology, and stratigraphy. Ann. Rev. Mar. Sci. 7, 67–88. https://doi.org/10.1146/annurev-marine-010213-135032.

Wilson, C., Goodbred, S., Small, C., Gilligan, J., Sams, S., Mallick, B., Hale, R., 2017. Widespread infilling of tidal channels and navigable waterways in the human-modified tidal deltaplain of southwest Bangladesh. Elementa 5. https://doi.org/10.1525/elementa.263.

Xia, X., Yue, W., Zhai, Y., Teng, Y., 2023. DOM accumulation in the hyporheic zone promotes geogenic Fe mobility: A laboratory column study. Sci. Total Environ. 896, 165140 https://doi.org/10.1016/j.scitotenv.2023.165140.